

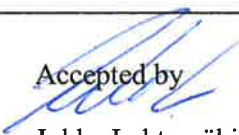


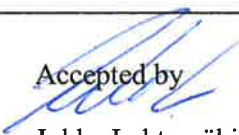


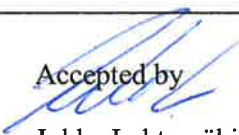


Characterisation of the produced particles by the IndMeas industrial flow calibration device – reagent and filter collection experiments

Authors: Jussi Lyyränen¹, Ville Laukkanen², Kenneth Ahlfors² and Ari Auvinen¹
1 VTT, P.O. Box 1000, FI-02044 VTT, Finland,
2 IndMeas, Tietäjäsentie 12, FI-02130 ESPOO, Finland

Confidentiality: Confidential

Report's title Characterisation of the produced particles by the IndMeas industrial flow calibration device – reagent and filter collection experiments				
Customer, contact person, address Ville Laukkanen IndMeas, Tietäjantie 12, FI-02130, Espoo, Finland	Order reference			
Project name Production and dispersion of tracer particles for process flow measurements	Project number/Short name 71091-1.4			
Author(s) Jussi Lyyränen ¹ , Ville Laukkanen ² , Kenneth Ahlfors ² and Ari Auvinen ¹	Pages 38			
Keywords Particle measurement, characterisation, flow calibration	Report identification code VTT-R-03689-12			
<p>Summary</p> <p>A measurement (calibration) device designed by the IndMeas company for the calibration of industrial flow meters with the help of activated particles was studied and characterised. With this device it is also possible to check/evaluate, e.g. emissions and energy balances of an industrial facility. During the first campaign (11/2010) different concentrations of $\text{Fe}(\text{NO}_3)_3 \cdot 9\text{H}_2\text{O}$ reagent were studied with and without added silica. The produced particles directly enter the measurement system without collection. During the second campaign (9/2011) the particles were collected after the production with a new filter sampler instead of a cyclone. Many different reagents and reagent combinations were tested.</p> <p>The mass size distribution for $\text{Fe}(\text{NO}_3)_3 \cdot 9\text{H}_2\text{O}$ with or without silica reagent were almost identical: mode at 72 nm, and major part of the particles were smaller than 1 μm. For BaCl_2 reagent the particles grew larger (mode at 2.7 μm). The individual particles for $\text{Fe}(\text{NO}_3)_3 \cdot 9\text{H}_2\text{O}$ reagent were different sized spheres the smallest being <200 nm. Silica caused the particles to be less spherical.</p> <p>The mass size distribution for filter collection with $\text{Fe}(\text{NO}_3)_3 \cdot 9\text{H}_2\text{O}$ and $\text{Fe}(\text{NO}_3)_3 \cdot 9\text{H}_2\text{O} + \text{Ba}(\text{NO}_3)_2$ reagent were clearly bimodal, and almost identical independent on the addition of $\text{Ba}(\text{NO}_3)_2$ reagent (modes at 70 nm and 6 μm). It seemed that the particles were agglomerating at the filter collection possibly because of the water condensation at the lower temperature than usual with the cyclone collection during the filter collection of the particles. It was also found that for continuous production nearly over 60 % of the mass of the particles was found in smaller than 1 μm sized particles. With the filter collection of the particles only 30 % of the mass was found in smaller than 1 μm sized particles.</p> <p>The solution to the agglomeration could be a higher collection temperature or another reagent or a “deagglomerating agent”. Another possibility would be to skip the particle collection phase totally, because the most severe agglomeration occurred during filter collection.</p>				
Confidentiality	{Public, Restricted, Confidential}			
Espoo 16.5.2012 <table border="0"> <tr> <td>Written by  Jussi Lyyränen Senior Scientist (D.Sc.)</td> <td>Reviewed by  Ari Auvinen Team leader</td> <td>Accepted by  Jukka Lehtomäki Technology manager</td> </tr> </table>		Written by  Jussi Lyyränen Senior Scientist (D.Sc.)	Reviewed by  Ari Auvinen Team leader	Accepted by  Jukka Lehtomäki Technology manager
Written by  Jussi Lyyränen Senior Scientist (D.Sc.)	Reviewed by  Ari Auvinen Team leader	Accepted by  Jukka Lehtomäki Technology manager		
VTT's contact address P.O. Box 1000, FI-02044 VTT, Finland				
Distribution (customer and VTT) {Customer, VTT and other distribution. In confidential reports the company, person and amount of copies must be named. Continue to next page when necessary.}				
<i>The use of the name of the VTT Technical Research Centre of Finland (VTT) in advertising or publication in part of this report is only permissible with written authorisation from the VTT Technical Research Centre of Finland.</i>				

Contents

1	Introduction.....	3
2	Methods.....	3
2.1	Principles of measurement devices	3
2.2	Studied process and measurement set-up.....	4
2.3	Experimental matrix	6
3	Results	8
3.1	Continuous production of particles, no collection device.....	8
3.1.1	Fe(NO ₃) ₃ ·9H ₂ O, Fe(NO ₃) ₃ ·9H ₂ O + silica and BaCl ₂ as a reference	8
3.1.1.1	Particle number concentration and number size distribution....	8
3.1.1.2	Particle mass concentration and mass size distribution	14
3.1.1.3	Particle morphology	17
3.2	Filter collection of produced particles.....	18
3.2.1	Fe(NO ₃) ₃ ·9H ₂ O and Fe(NO ₃) ₃ ·9H ₂ O + Ba(NO ₃) ₂	18
3.2.1.1	Particle number concentration and number size distribution..	18
3.2.1.2	Particle mass concentration and mass size distribution	22
3.2.1.3	Particle morphology	24
3.2.2	Ba(NO ₃) ₂ , BaCl ₂ , Ba(NO ₃) ₂ +Al(NO ₃) ₃ and Fe(NO ₃) ₃ ·9H ₂ O+NaNO ₃ ..	27
3.2.2.1	Particle number concentration and number size distribution..	27
3.2.2.2	Particle mass concentration	30
3.2.2.3	Particle morphology	32
4	Summary and conclusions.....	34
	References	37

1 Introduction

This study titled as “Production and dispersion of tracer particles for process flow measurements” is a part of the CLEEN MMEA (Measurement, monitoring and environmental efficiency assessment) research program going on during 2010-2014. The aim of the research program is “to combine the development of new measurement technologies, data quality assurance methods, modelling and forecasting tools, and information and communication technology (ICT) infrastructure (CLEEN MMEA factsheet, 2010).”

A measurement (calibration) device designed by the IndMeas company for the calibration of industrial flow meters with the help of activated particles is studied and characterised. With this device it is also possible to check/evaluate, e.g. emissions and energy balances of an industrial facility. The method applies ^{137}Ba -tracer, whose $t_{d,1/2}=153$ s. The aim of the research is to characterise the IndMeas-measurement method and to improve its performance. The main focus is to concentrate on thoroughly characterising the particles produced by the device with different reagents, and on improving the properties of the particles, i.e. to reduce their adherence and decrease their size to reduce particle losses by, e.g. deposition.

2 Methods

2.1 Principles of measurement devices

In the following section a short description of the experimental techniques and equipment used in this study is provided. For more thorough information the required references are provided.

An aspiration electron microscopy sampler (AEM sampler) was used to collect samples for morphology studies in scanning electron microscope (SEM). The sampler consists of an EM grid mounting head soldered with silver into 6 mm tubing and Swagelok fittings. The carbon coated copper grid (Holey carbon, $d_{\text{grid}}=3.1$ mm) is mounted on the grid mounting head with the help of a hollow screw, and a copper seal is mounted between the screw and the EM grid. The flow through the aspiration sampler is regulated to approximately 0.2 Nlpm with a critical orifice (CO). This sampler is designed and manufactured by VTT.

A Berner-type low-pressure Impactor (BLPI) was used to measure the mass size distribution of the particles. The BLPI has a total of 11 collection stages, where the aerosol is directed through orifices lying against a flat collection plate. The uppermost stage (11) collects particles whose Stokes diameter is larger than $10\ \mu\text{m}$ and the lowest stage (1) particles whose Stokes diameter is $0.01\text{-}0.02\ \mu\text{m}$. When passing through several successive impactor stages the aerosol is classified into several different size classes (Berner and Lürzer, 1980; Berner et al., 1979; Hillamo and Kauppinen, 1991; Kauppinen, 1992).

An electrical low-pressure impactor (ELPI) was used to measure the particle number concentration and number size distribution. The base of the ELPI is a 12 stage cascade low-pressure impactor with a without a final filter stage. In these measurements the ELPI is equipped with a filter stage. In ELPI the particles are charged with a unipolar diode charger to a well-defined charge level prior entering the cascade impactor. Inside the impactor the particles are classified in to 12 size classes (from 30 nm to 10 μm) according to their aerodynamic diameter. When collected at the different collection stages the particles produce electric current that is measured with highly sensitive electrometers. The results may then be recorded to a PC equipped with a control software (Keskinen, et al., 1992; Baltensperger, Weingartner, Burtscher and Keskinen, 2001).

A tapered element oscillating microbalance (TEOM). A 1400a-type TEOM (Patashnick and Rupprecht, 1986; Patashnick and Rupprecht, 1991) was used to measure continuously the particle mass concentration. The particles were collected on a filter, which was placed on top of a transversely vibrating hollow rod. The sample flow was drawn through the filter and the rod with a pump. Because the rod oscillates as a harmonic oscillator the mass of the oscillating element (the hollow rod and the filter) can be calculated from the vibration frequency of the rod.

A porous tube diluter (PRD, dilution probe) was used to reduce particle deposition and total particle concentration suitable for the measurement devices. PRD is a coaxial cylindrical diluter in which the dilution air flows through a porous tube (pore size 20 μm) into the inner tube, thus sheeting the aerosol flow from deposition and thermophoresis (Auvinen et al., 2000).

2.2 Studied process and measurement set-up

The operation principles IndMeas flow calibrator device (FCD) are described in the research report (Lyyräinen, et al., 2011). In this study the cyclone used for collection of the produced particles is either removed completely (Fig. 1a) to allow the produced particles directly enter the measurement system or the particles are collected on the surface of a filter and removed by a fast and powerful "blow" similar as in the case of the cyclone (Fig. 1b and c).

To characterise the particles produced with different reagents by the flow calibrator device (FCD) a measurement campaign was carried out to determine the particle number and mass concentration and number and mass size distribution and particle morphology and composition. During the first measurement campaign (**11/2010**) the produced particles entered directly the measurement system without being collected by any device (2a). This was carried out to find out the actual produced particle size by the FCD without being changed at the possible collection of the particles by, e.g. cyclone or filter.

During the second campaign (**9/2011**) the produced particles were collected on the surface of a custom made filter and "blown" away with air (Fig. 1b and c). The particles were sampled directly from the exhaust connection of the FCD (Fig. 1b,c and 2b). To maintain the temperature of the filter high enough to avoid condensation it was heated with a thermal band and insulated. The temperature was set to 130 °C.

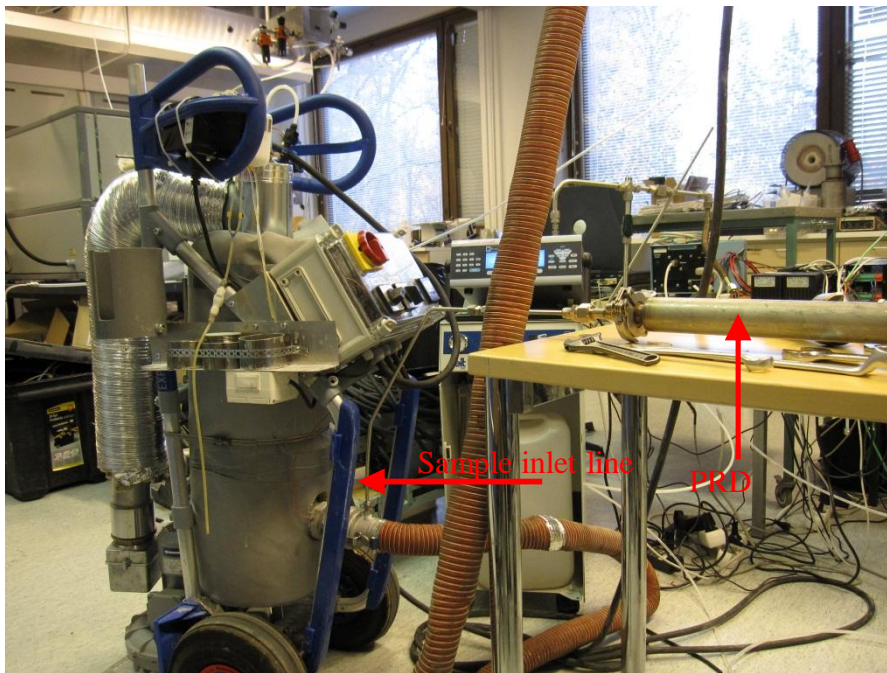


Fig.1a. Measurements set-up for continuous production of the particles without any collection device (11/2010).

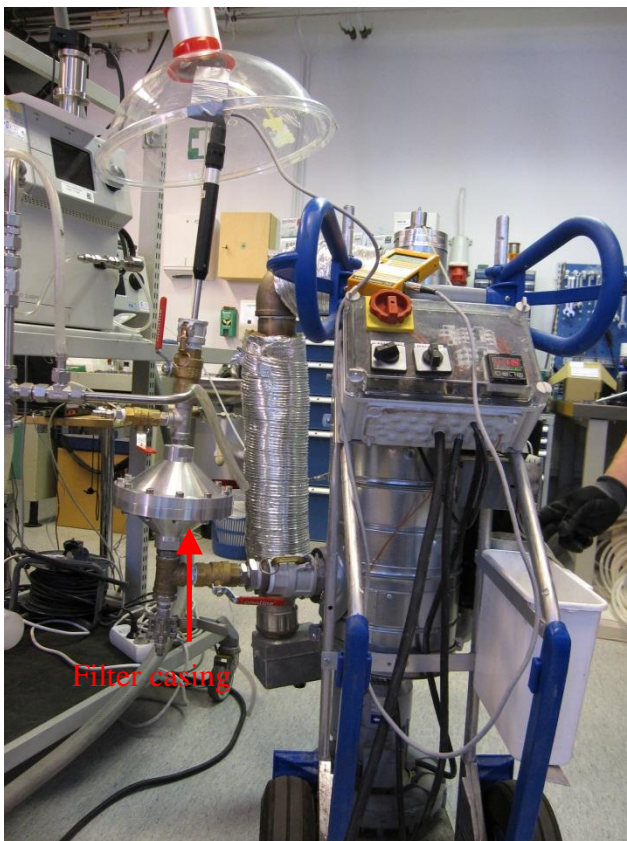


Fig.1b. Measurements set-up for filter collection of the produced particles (09/2011).



Fig. 1c. Measurements set-up for filter collection of the produced particles (09/2011).

In both sampling cases the aerosol flow (produced particles) from the FCD was diluted with a porous tube diluter (PRD; Fig. 2a and 2b) in order to reduce particle deposition and total particle concentration suitable for the measurement devices. The dilution gas was air, and the dilution flow was set to 80 Nlpm, and controlled

with a Brooks 5800-series mass flow meter. A digital pressure gauge and temperature meter were also installed in the sampling line to find out the possible pressure peak caused by the “particle blow” from the cyclone collection cup. To ensure adequate mixing of the aerosol flow from the FCD and the dilution air the length of the sampling line was set to >0.5 m. In addition, a by-pass line was also installed in the sampling line to pass the “excess” flow not aspirated by the measurement devices to the exit (Fig. 2a and 2b).

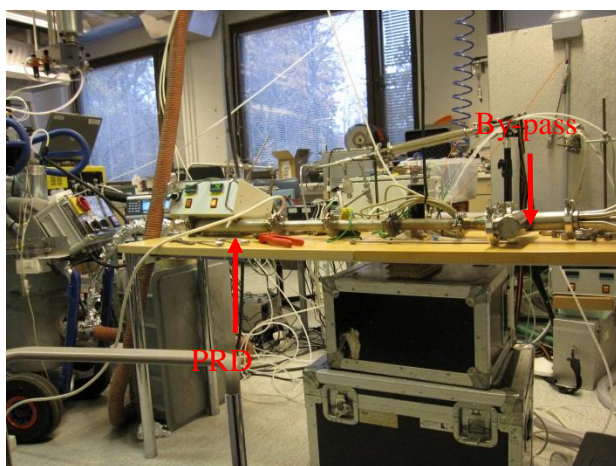


Fig. 2a. Measurement set-up for the particle characterisation measurements during campaign 11/2010.

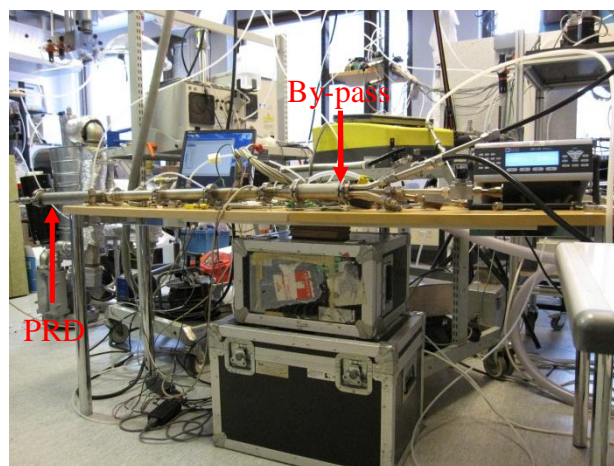


Fig. 2b. Measurement set-up for the particle characterisation measurements during campaign 9/2011.

2.3 Experimental matrix

The experimental matrix was roughly divided into two parts:

- The characterisation of produced particles with different reagents using continuous production (11/2010) of the particles without collecting them, i.e. all the produced particles are directly entered the measurement system without being collected first and then “blown” to the system with a powerful air/ N_2 blow. Studied reagents were iron nitrate in various concentrations with added silica and barium chloride (Table 1).
- The characterisation of produced particles with different reagents by collecting the particles on the surface of a filter and then “blown” away by a powerful air blow (9/2011). The studied reagents were different nitrates and barium chloride (Table 2).

Table 1. Measurement matrix for 11/2010 campaign. Used reagents, processes (charges (pulses) or continuous production), BLPI and electron microscopy sample collection times. Reagent concentration and feed rate are also given.

Date	Reagent(s)	Time	Process	BLPI	SEM
1.11.2010	Fe(NO ₃) ₃ ·9H ₂ O 20 g/dm ³ , 20 ml/min	12:29-12:36	Continuous		
	Fe(NO ₃) ₃ ·9H ₂ O 10 g/dm ³ , 20 ml/min	12:42-12:51			
	Fe(NO ₃) ₃ ·9H ₂ O 40 g/dm ³ , 20 ml/min	12:56-13:03			
	Fe(NO ₃) ₃ ·9H ₂ O+Si 20 g/dm ³ , 10 ml/min	13:14-13:19			
	Fe(NO ₃) ₃ ·9H ₂ O 20 g/dm ³ , 10 ml/min	13:20-13:26			
	Fe(NO ₃) ₃ ·9H ₂ O 20 g/dm ³ , 10 ml/min	13:50-13:55			
	Fe(NO ₃) ₃ ·9H ₂ O 20 g/dm ³ , 20 ml/min	13:56-14:02			
2.11.2010	Fe(NO ₃) ₃ ·9H ₂ O 80 g/dm ³ , 20 ml/min	12:43-12:51	Continuous		
	Fe(NO ₃) ₃ ·9H ₂ O+Si 80 g/dm ³ , 20 ml/min	12:52-12:58			
	Fe(NO ₃) ₃ ·9H ₂ O 20 g/dm ³ , 20 ml/min	13:11-13:20			
	Fe(NO ₃) ₃ ·9H ₂ O+Si 20 g/dm ³ , 20 ml/min	13:21-13:28			
	Fe(NO ₃) ₃ ·9H ₂ O 40 g/dm ³ , 20 ml/min	13:29-13:35			
	Fe(NO ₃) ₃ ·9H ₂ O+Si 40 g/dm ³ , 20 ml/min	13:36-13:44			
3.11.2010	Fe(NO ₃) ₃ ·9H ₂ O 40 g/dm ³ , 20 ml/min	12:39-13:26	Continuous	13:04-13:24	13:16
4.11.2010	Fe(NO ₃) ₃ ·9H ₂ O+Si 40 g/dm ³ , 20 ml/min	12:52-13:26	Continuous	13:06-13:26	13:15
	BaCl ₂ , 11 g/dm ³	13:44-14:29	Continuous	14:00-14:28	14:06

Table 2. Measurement matrix for 09/2011 campaign. Used reagents, processes (charges (pulses) or continuous production), BLPI and electron microscopy sample collection times. Reagent concentration and feed rate are also given.

Date	Reagent(s)	Time	Process	BLPI	SEM
30.8.2011	Fe(NO ₃) ₃ ·9H ₂ O 40 g/dm ³ , 15 ml/min	14:12-14:28	Charges (3)		
	No reagent feed	14:40-14:56	Charges (3)		
	Fe(NO ₃) ₃ ·9H ₂ O 40 g/dm ³ + Ba(NO ₃) ₂ , 15+4 ml/min	15:15-15:39	Charges (4)		
	No reagent feed	15:46-15:53	Charges (2)		
31.8.2011	Fe(NO ₃) ₃ ·9H ₂ O 50 g/dm ³ , 15 ml/min	13:53-14:15	Charges (9)	14:04-14:18	14:08
	No reagent feed	14:23-14:26	Charges (3)		
	Fe(NO ₃) ₃ ·9H ₂ O 50 g/dm ³ + Ba(NO ₃) ₂ , 1 g/ dm ³	14:33-14:56	Charges (9)	14:42-15:01	14:47
	Fe(NO ₃) ₃ ·9H ₂ O 40 g/dm ³ + Ba(NO ₃) ₂ , 10 g/ dm ³	15:11-15:31	Charges (9)	15:16-15:35	15:21
	No reagent feed	15:37-15:39	Charges (3)		
1.9.2011	Ba(NO ₃) ₂ , 50 g/dm ³ , 4 ml/min	12:53-13:26	Charges (4)		13:07
	No reagent feed	13:20	Charges (2)		
	BaCl ₂ , 50 g/dm ³ , 4 ml/min	13:29-13:54	Charges (5)		13:48
	No reagent feed	14:01-14:08	Charges (2)		
	Fe(NO ₃) ₃ ·9H ₂ O 40 g/dm ³ + NaNO ₃ , 10 g/ dm ³	14:15-14:41	Charges (5)		14:34
	No reagent feed	14:47	Charges (1)		
	Ba(NO ₃) ₂ ·9H ₂ O 25 g/dm ³ + Al(NO ₃) ₃ , 25 g/ dm ³	14:59-15:24	Charges (5)		15:19
	No reagent feed	15:31	Charges (1)		

3 Results

3.1 Continuous production of particles, no collection device

3.1.1 Fe(NO₃)₃·9H₂O, Fe(NO₃)₃·9H₂O + silica and BaCl₂ as a reference

3.1.1.1 Particle number concentration and number size distribution

Particle number concentration and size distribution was measured with an ELPI. Typical particle number concentration during the continuous particle generation

(no collection device) with **Fe(NO₃)₃·9H₂O reagent** (20 g/dm³, 20 ml/min) varied between 3.0-4.0·10⁵ 1/cm³, and the aerodynamic count median diameter (CMD_{ae}) of the particles varied from 70 to 100 nm (Fig. 3). With half of the concentration but the same feed rate (10 g/dm³, 20 ml/min) the number concentration was 3.0-3.2·10⁵ 1/cm³, and the aerodynamic count median diameter (CMD_{ae}) of the particles varied from 65 to 80 nm (Fig. 3). Doubling the concentration (40 g/dm³, 10 ml/min) increased the number concentration to 4.4-6.3·10⁵ 1/cm³, and the aerodynamic count median diameter (CMD_{ae}) of the particles varied from 66 to 75 nm (Fig. 3). With 20 g/dm³, 10 ml/min and with the **added silica** number concentration increased significantly to 7.1·10⁶ 1/cm³, and aerodynamic count median diameter (CMD_{ae}) of the particles varied from 55 to 60 nm.

The number size distribution (NSD) with **Fe(NO₃)₃·9H₂O** reagent with different concentrations during continuous collection of the particles (no collection device) was typically almost unimodal with a peak at approx. 40 and 70 nm depending on reagent concentration and feed rate. However, indication of a bimodal character was also observed in some cases. With **added silica** the number size distribution became seemingly wider than without silica (Fig. 4). The number concentration was also a decade or higher with silica than without it. This indicated change in particle size and possibly in morphology.

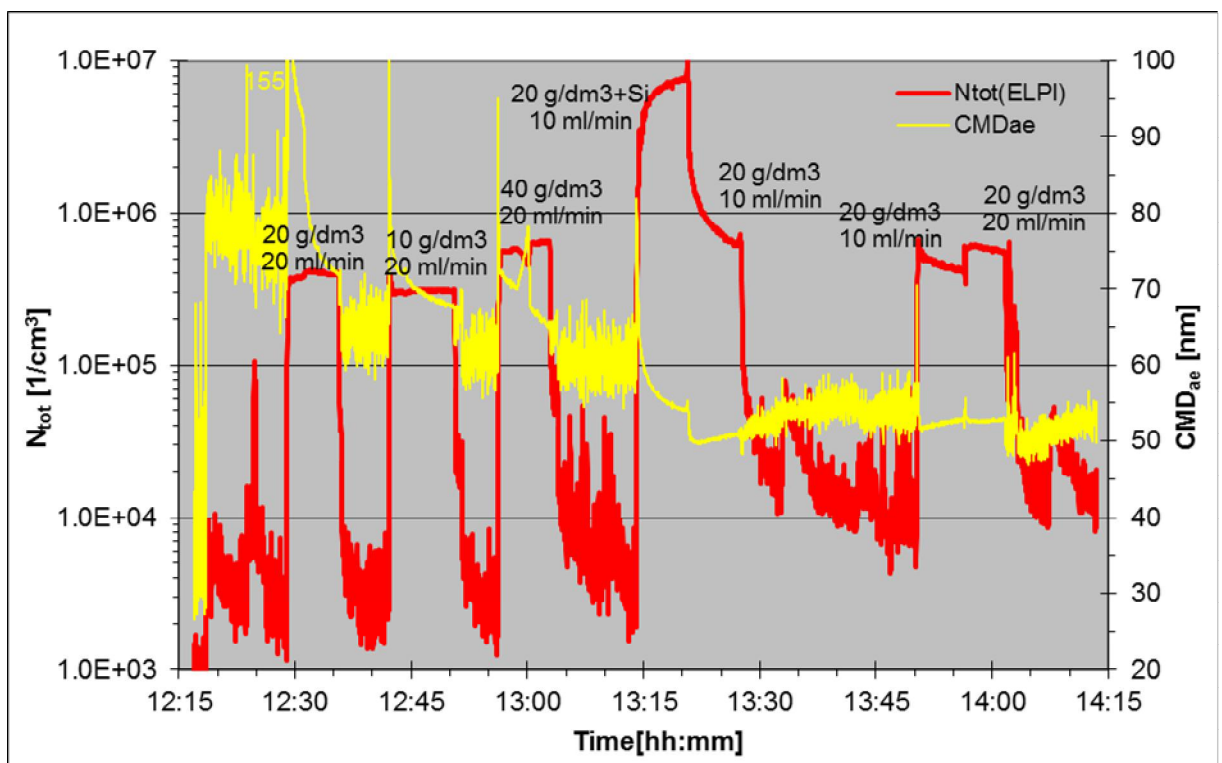


Fig. 3. Total particle number concentration and aerodynamic count median diameter (CMD_{ae}) of the particles generated from Fe(NO₃)₃·9H₂O + silica reagent measured with ELPI on 1.11. 2010, continuous production of particles, no collection device.

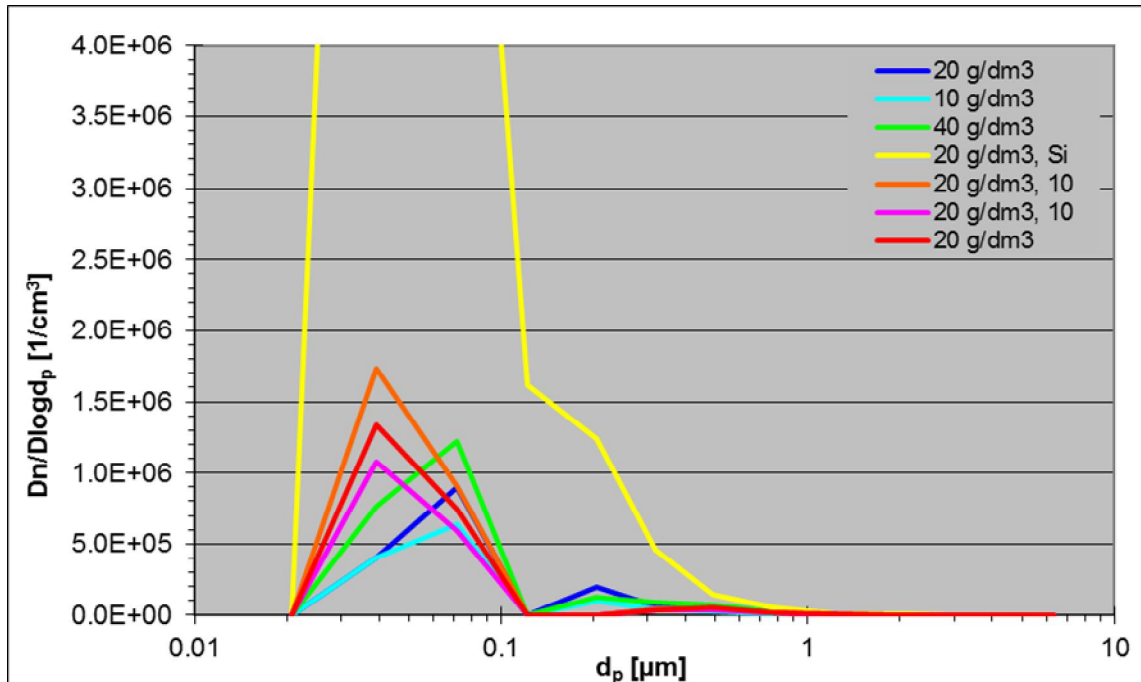


Fig. 4. Average number size distributions for the particles generated from $\text{Fe}(\text{NO}_3)_3 \cdot 9\text{H}_2\text{O}$ + silica reagent measured with ELPI on 1.11. 2010, continuous production of particles, no collection device (see Fig. 3; 10=10 ml/min reagent feed, others 20 ml/min).

With $\text{Fe}(\text{NO}_3)_3 \cdot 9\text{H}_2\text{O}$ reagent with 80 g/dm^3 during continuous particle generation (no collection device) the particle number concentration varied $0.9\text{--}1.5 \cdot 10^6 \text{ 1/cm}^3$, and the aerodynamic count median diameter (CMD_{ae}) of the particles varied from 65 to 67 nm (Fig. 5). **Adding silica** increased number concentration up to $3.8 \cdot 10^6 \text{ 1/cm}^3$, and the aerodynamic count median diameter (CMD_{ae}) of the particles varied from 53 to 63 nm (Fig. 5). For concentrations 20 g/dm^3 and 40 g/dm^3 almost similar results as before (1.11.2010) were obtained when the error limits of the measurements are taken into account.

The number size distribution (NSD) with $\text{Fe}(\text{NO}_3)_3 \cdot 9\text{H}_2\text{O}$ reagent with different concentrations during continuous collection of the particles (no collection device) was typically almost unimodal with a peak at approx. 40 and 50 nm. However, indications of a bimodal character were also observed in some cases. With **added silica** the number size distribution became wider, and the total number concentration much higher than without silica (Fig. 4).

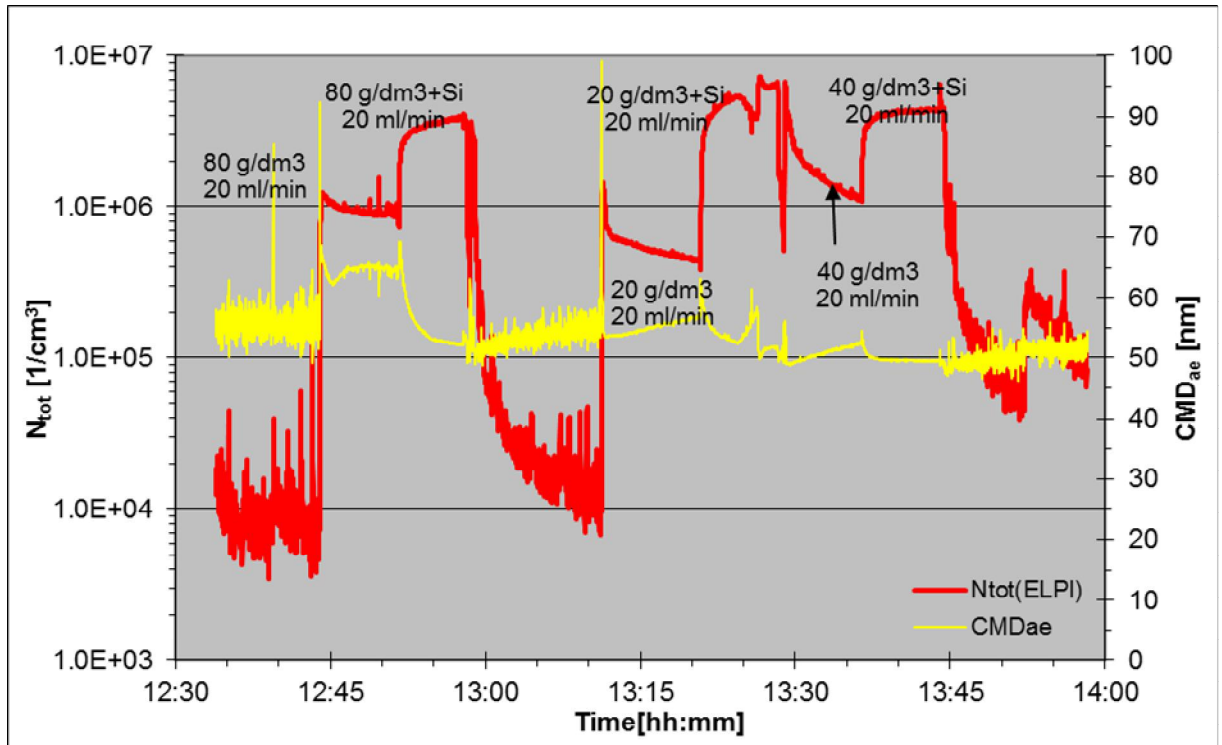


Fig. 5. Total particle number concentration and aerodynamic count median diameter (CMD_{ae}) of the particles generated from $Fe(NO_3)_3 \cdot 9H_2O$ + silica reagent measured with ELPI on 2.11. 2010, continuous production of particles, no collection device.

Based on previous “screening studies” (experiments on 1.11.2010 and 2.11.2010) it was decided to study the $Fe(NO_3)_3 \cdot 9H_2O$ and $Fe(NO_3)_3 \cdot 9H_2O$ + silica reagents in more detail: measuring the mass size distribution for these reagents and taking electron microscopy samples for morphology and composition analyses (to be presented in following chapters). The number concentration measured with ELPI for $Fe(NO_3)_3 \cdot 9H_2O$ (40 g/dm³, 20 ml/min) reagent varied from $1.5 \cdot 10^6$ 1/cm³ to $0.4 \cdot 10^6$ 1/cm³ thus decreasing as a function of time, and the aerodynamic count median diameter (CMD_{ae}) of the particles varied from 52 to 61 nm (Fig. 7).

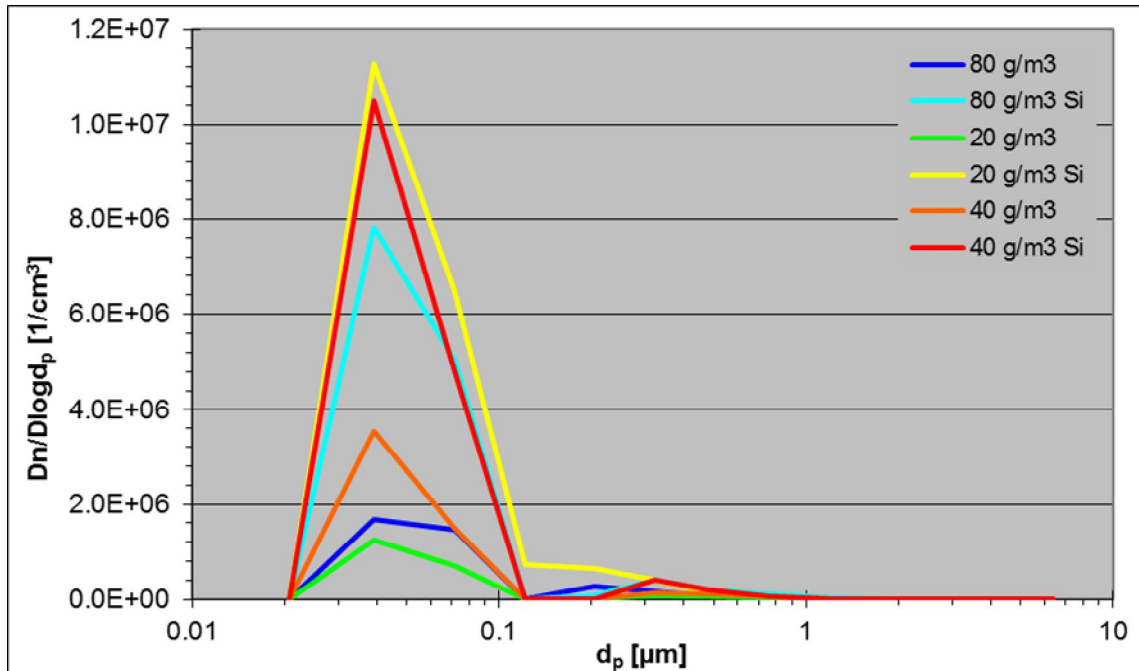


Fig. 6. Average number size distributions for the particles generated from $\text{Fe}(\text{NO}_3)_3 \cdot 9\text{H}_2\text{O}$ + silica reagent measured with ELPI on 2.11. 2010, continuous production of particles, no collection device (see Fig. 4).

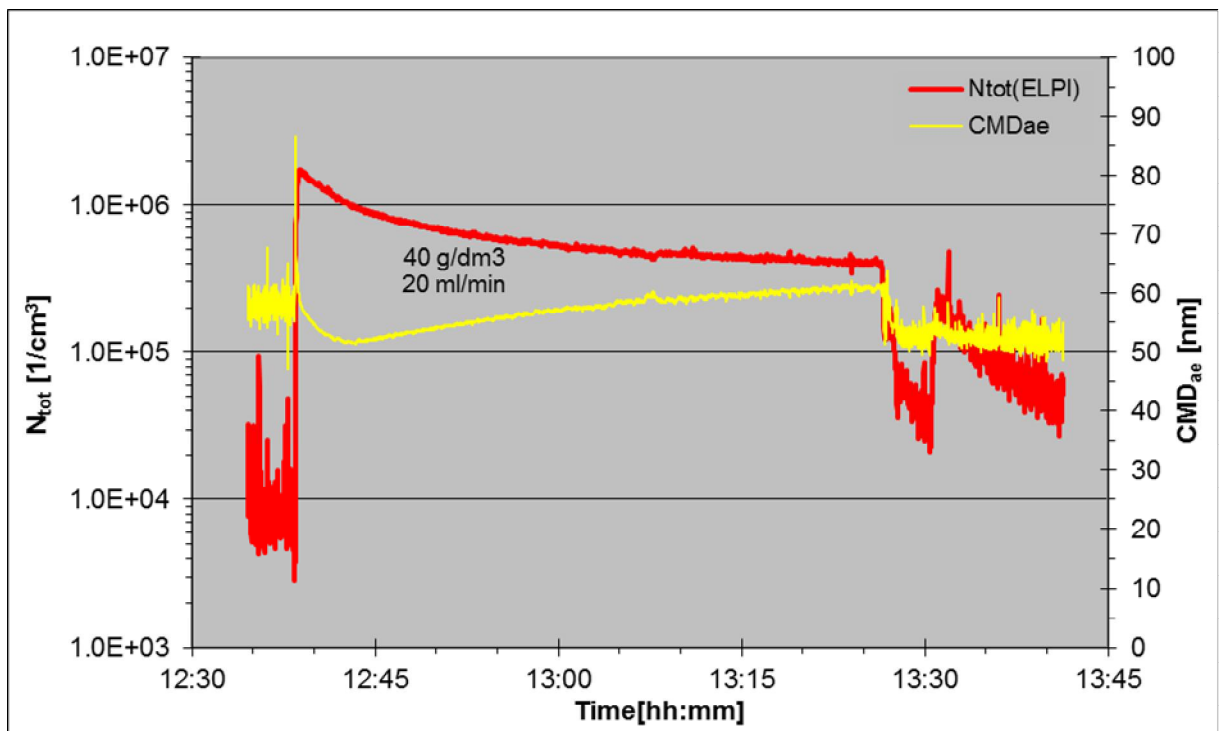


Fig. 7. Total particle number concentration and aerodynamic count median diameter (CMD_{ae}) of the particles generated from $\text{Fe}(\text{NO}_3)_3 \cdot 9\text{H}_2\text{O}$ reagent measured with ELPI on 3.11. 2010, continuous production of particles, no collection device.

The mode (approximately 40 nm) in the number size distribution remained the same despite of the decrease in the number concentration. The shape the distribution became narrower as a function of time, and had a small second mode at approximately $0.32 \mu\text{m}$ (Fig. 8).

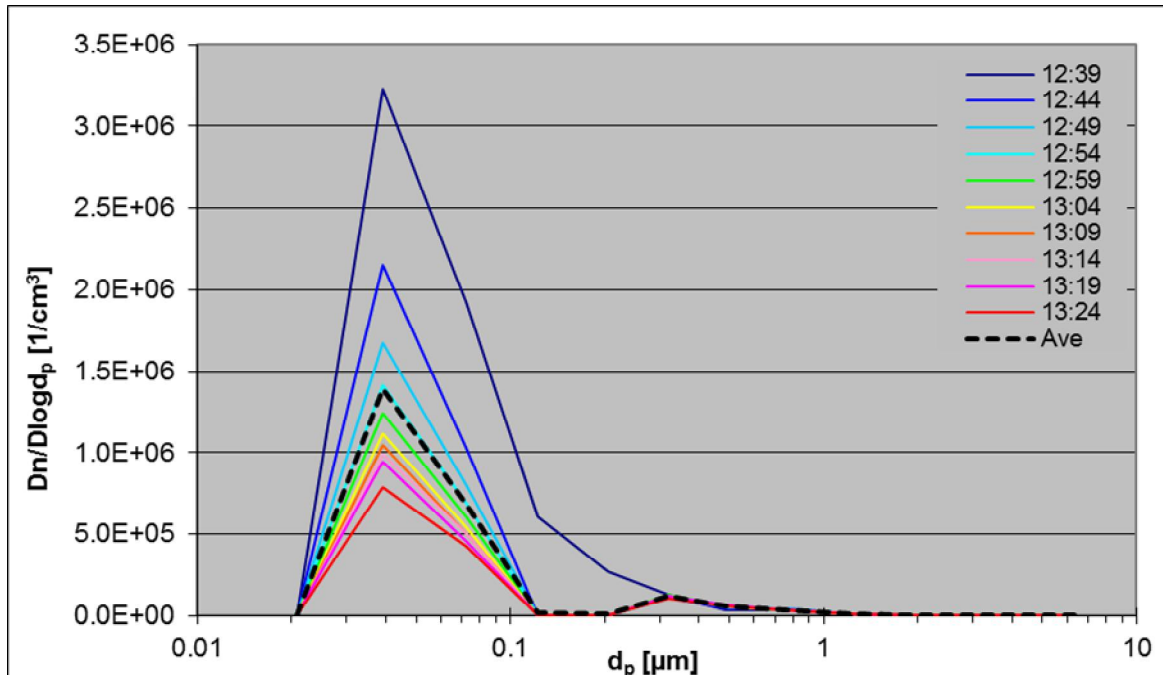


Fig. 8. Evolution of particle number size distribution and average number size distribution (black broken line) for the particles generated from $\text{Fe}(\text{NO}_3)_3 \cdot 9\text{H}_2\text{O}$ reagent measured with ELPI on 3.11. 2010, continuous production of particles, no collection device (see Fig. 7).

For $\text{Fe}(\text{NO}_3)_3 \cdot 9\text{H}_2\text{O}$ + silica (40 g/dm^3 , 20 ml/min) reagent the number concentration varied from $3.0 \cdot 10^6 \text{ 1/cm}^3$ to $5.5 \cdot 10^6 \text{ 1/cm}^3$, and the aerodynamic count median diameter (CMD_{ae}) of the particles varied from 51 to 66 nm (Fig. 9). Thus the number concentration was 5-10 times higher than without the added silica.

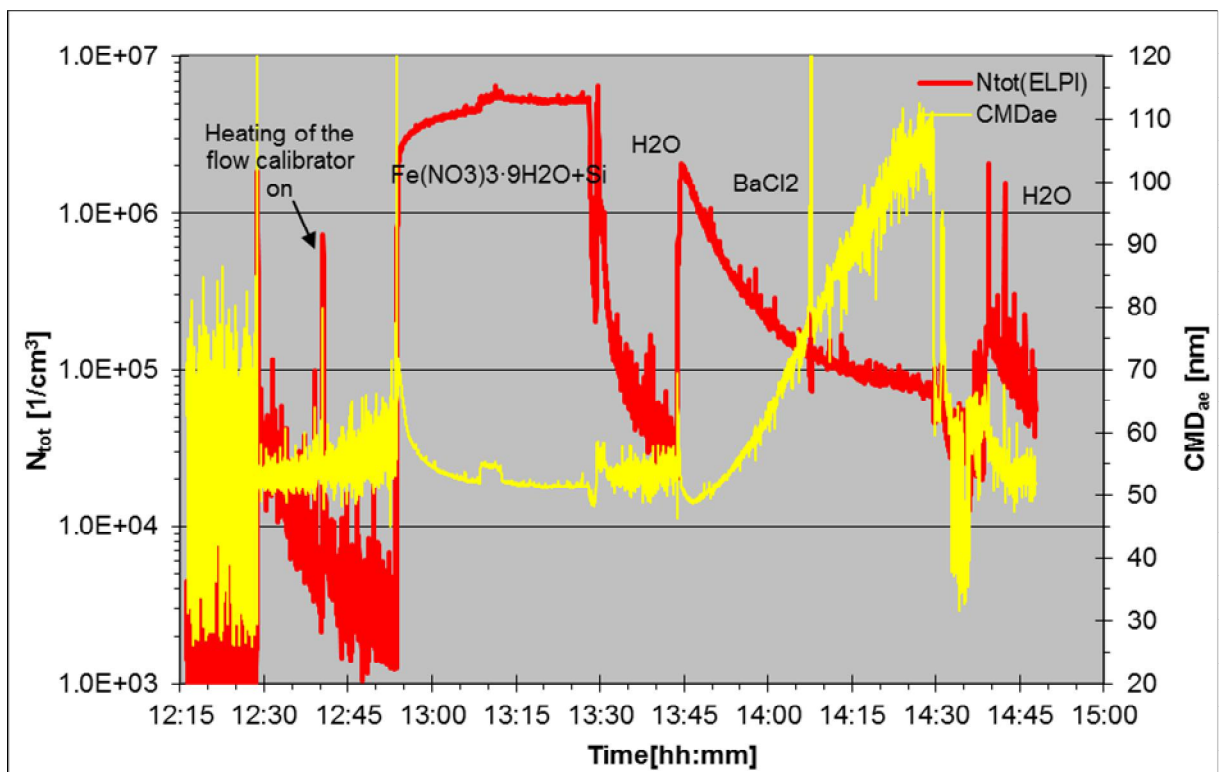


Fig. 9. Total particle number concentration and aerodynamic count median diameter (CMD_{ae}) of the particles generated from $\text{Fe}(\text{NO}_3)_3 \cdot 9\text{H}_2\text{O}$ + silica and BaCl_2 reagent

measured with ELPI on 4.11. 2010, continuous production of particles, no collection device.

For BaCl_2 reagent the number concentration decreased steadily from $1.7 \cdot 10^6$ $1/\text{cm}^3$ to $0.8 \cdot 10^6$ $1/\text{cm}^3$, and the aerodynamic count median diameter (CMD_{ae}) of the particles varied from 51 to 108 nm (Fig. 9). Thus the number concentration with BaCl_2 was roughly about the same as with $\text{Fe}(\text{NO}_3)_3 \cdot 9\text{H}_2\text{O}$ without the silica (Fig. 7).

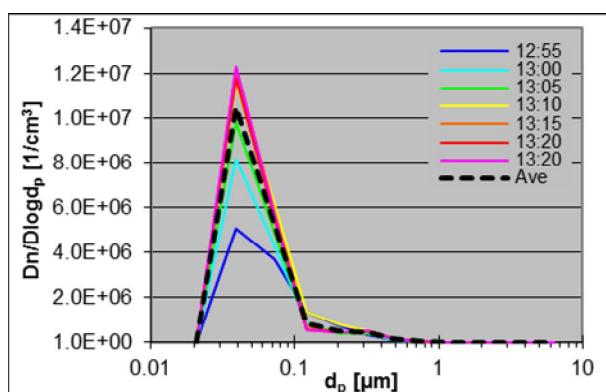


Fig. 10a. Evolution of particle number size distribution and average number size distribution (black broken line) for the particles generated from $\text{Fe}(\text{NO}_3)_3 \cdot 9\text{H}_2\text{O}$ + silica reagent measured with ELPI on 4.11. 2010, continuous production of particles, no collection device (see Fig. 9)

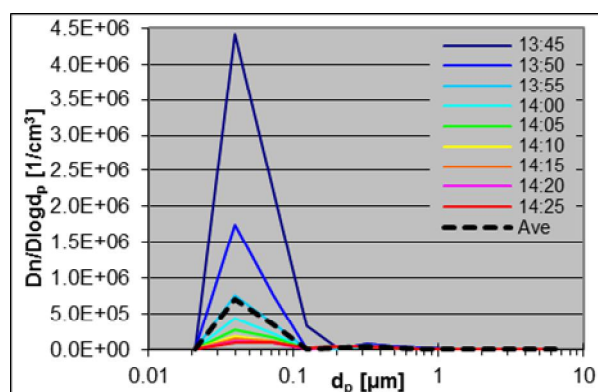


Fig. 10b. Evolution of particle number size distribution and average number size distribution (black broken line) for the particles generated from BaCl_2 reagent measured with ELPI on 4.11. 2010, continuous production of particles, no collection device (see Fig. 9)

The number size distribution for $\text{Fe}(\text{NO}_3)_3 \cdot 9\text{H}_2\text{O}$ + silica (Fig. 10a) had the mode at the same location as without the silica (Fig. 8), at approximately 40 nm. The number size distributions were almost similar in shape, thus it seems that the particle size did not change with the added silica. It has to be, though, remembered that the size resolution of the ELPI is not very sensitive to small particle size changes (on the order of tens of nm).

For BaCl_2 reagent the mode is again in the 40 nm sized particles (Fig. 10b). The number size distributions were almost similar in shape to those measured for $\text{Fe}(\text{NO}_3)_3 \cdot 9\text{H}_2\text{O}$ (Fig. 8) and $\text{Fe}(\text{NO}_3)_3 \cdot 9\text{H}_2\text{O}$ + silica (Fig. 10a). It thus suggests that the particle size did not change much with changed reagent. It has to be, though, remembered that the size resolution of the ELPI is not very sensitive to small particle size changes (on the order of tens of nm).

3.1.1.2 Particle mass concentration and mass size distribution

The particle mass concentration was measured online with TEOM. The particle mass concentration during the continuous particle generation (no collection device) with $\text{Fe}(\text{NO}_3)_3 \cdot 9\text{H}_2\text{O}$ reagent ($20 \text{ g}/\text{dm}^3$, $20 \text{ ml}/\text{min}$) was approximately $7 \text{ mg}/\text{m}^3$ (Fig. 11a). With half of the reagent concentration ($10 \text{ g}/\text{dm}^3$, $20 \text{ ml}/\text{min}$) the mass concentration decreased to approximately $4 \text{ mg}/\text{m}^3$. Doubling the concentration from the base case to $40 \text{ mg}/\text{dm}^3$ increased the measured mass concentration to approximately $11 \text{ mg}/\text{m}^3$. With $20 \text{ g}/\text{dm}^3$, $10 \text{ ml}/\text{min}$ and with the **added**

silica the mass concentration increased to approximately 9 mg/m^3 . Thus the added silica increased the mass concentration approximately 30 %.

With **$\text{Fe}(\text{NO}_3)_3 \cdot 9\text{H}_2\text{O}$ reagent** with 80 g/dm^3 during continuous particle generation (no collection device) the particle mass concentration varied between $17\text{--}19 \text{ mg/m}^3$ (Fig. 11b). Adding **silica** increased the mass concentration to approximately 27 mg/m^3 . With 20 g/dm^3 the number concentration decreased to approximately 7 mg/m^3 as measured before (Fig. 11a). With added silica the number concentration increased to approximately 10 mg/m^3 , which was about the as measured before (Fig. 11a). With 40 mg/dm^3 concentration the measured mass concentration was approximately 12 mg/m^3 , as was also found in previous measurements (Fig. 11a). With the **added silica** the mass concentration increased to 16 mg/m^3 , thus approximately 25 %.

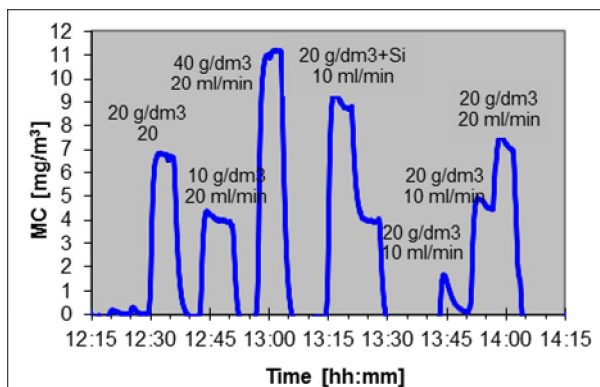


Fig. 11a. Particle mass concentration for the particles generated from $\text{Fe}(\text{NO}_3)_3 \cdot 9\text{H}_2\text{O}$ + silica reagent measured with TEOM on 1.11. 2010, continuous production of particles, no collection device.

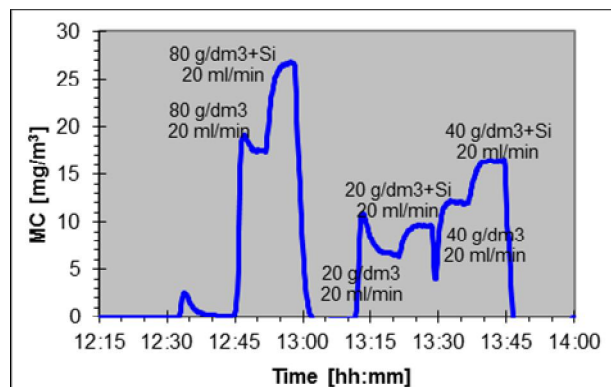


Fig. 11b. Particle mass concentration for the particles generated from $\text{Fe}(\text{NO}_3)_3 \cdot 9\text{H}_2\text{O}$ + silica reagent measured with TEOM on 2.11. 2010, continuous production of particles, no collection device (see Fig. 9)

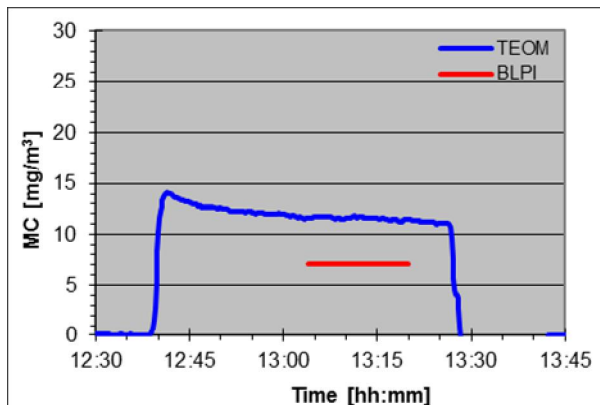


Fig. 11c. Particle mass concentration for the particles generated from $\text{Fe}(\text{NO}_3)_3 \cdot 9\text{H}_2\text{O}$ reagent measured with TEOM on 3.11. 2010, continuous production of particles, no collection device.

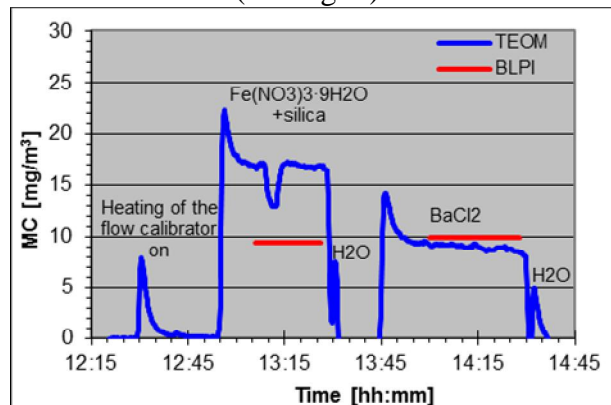


Fig. 11d. Particle mass concentration for the particles generated from $\text{Fe}(\text{NO}_3)_3 \cdot 9\text{H}_2\text{O}$ + Si and BaCl_2 reagent measured with TEOM on 4.11. 2010, continuous production of particles, no collection device.

Based on previous “screening studies” (experiments on 1.11.2010 and 2.11.2010) it was decided to study the $\text{Fe}(\text{NO}_3)_3 \cdot 9\text{H}_2\text{O}$ and $\text{Fe}(\text{NO}_3)_3 \cdot 9\text{H}_2\text{O}$ + silica reagents in more detail: measuring the mass size distribution for these reagents and taking electron microscopy samples for morphology and composition analyses. The mass concentration for **$\text{Fe}(\text{NO}_3)_3 \cdot 9\text{H}_2\text{O}$ reagent** measured with TEOM (40 g/dm^3 , 20

ml/min) varied from 11 mg/m^3 to 14 mg/m^3 (Fig. 11c). The mass concentration measured with BLPI was 7 mg/m^3 , approximately 64 % of that measured with TEOM.

For $\text{Fe}(\text{NO}_3)_3 \cdot 9\text{H}_2\text{O}$ + silica reagent measured with TEOM (40 g/dm^3 , 20 ml/min) the mass concentration was approximately 16 mg/m^3 , and for BLPI 9.4 mg/m^3 . For BaCl_2 reagent measured with TEOM the mass concentration was approximately 9 mg/m^3 , and for BLPI 9.9 mg/m^3 . The difference in measured mass concentration may have something to do with the chemical nature of the particles, because in some cases the consistency of the results between BLPI and TEOM are good and sometimes less good. This was also found here with using different reagents.

The mass size distribution for continuous production of particles (no collection device) with $\text{Fe}(\text{NO}_3)_3 \cdot 9\text{H}_2\text{O}$ and $\text{Fe}(\text{NO}_3)_3 \cdot 9\text{H}_2\text{O}$ + silica reagent were almost identical: the mode was at approximately 72 nm sized particles, and major part of the particles were smaller than $1 \mu\text{m}$ in aerodynamic size (assuming unit density of the particles). For BaCl_2 reagent the particles grew larger, and had a mode at approximately $2.7 \mu\text{m}$. For comparison, a mass size distribution from previous experiment (05/2010) for BaCl_2 reagent with cyclone collection followed by a “blow” had a mode at $1.4 \mu\text{m}$, at clearly smaller particles than for the continuous collection. The mass concentration was over two times higher with the cyclone collection. It is possible that the powerful “blow” through the cyclone partly caused the particles to disintegrate into smaller ones than with the continuous collection. On the other hand, one would assume that cyclone collection would also cause some agglomeration of the particles.

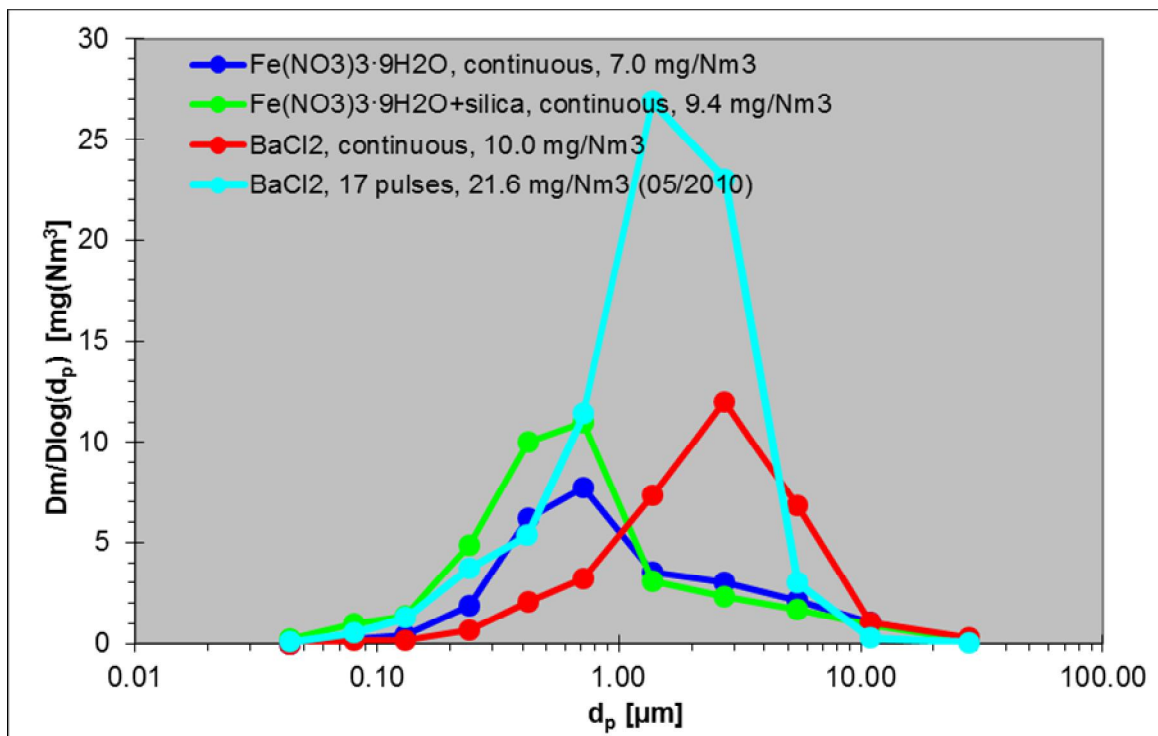


Fig. 12. Particle mass size distribution of the particles generated from $\text{Fe}(\text{NO}_3)_3 \cdot 9\text{H}_2\text{O}$ + silica and BaCl_2 reagent measured with BLPI during campaign 11/2010, continuous production of particles, no collection device. For comparison, a BaCl_2 mass size distribution with cyclone collection followed by a “blow” from earlier measurements (05/2010) has been added.

3.1.1.3 Particle morphology

The individual particle samples were collected with an aspiration electron microscopy sampler (AEM sampler). With the $\text{Fe}(\text{NO}_3)_3 \cdot 9\text{H}_2\text{O}$ reagent during continuous production of particles (no collection device) the particles were different sized spheres up to about few μm in diameter (Fig. 13a). The surface of the spheres was folded and wrinkled, and the smallest spherical particles were <200 nm in diameter (Fig. 13b). Adding silica to $\text{Fe}(\text{NO}_3)_3 \cdot 9\text{H}_2\text{O}$ reagent caused the particles to be less spherical, and the surface was not as smooth as without silica (Fig. 14a). The surface of the particles consisted partly of smaller almost spherical particles and cobblestone like structure (Fig. 14b). With BaCl_2 reagent the produced particles were different sized spheres (Fig. 15a) as in the case for $\text{Fe}(\text{NO}_3)_3 \cdot 9\text{H}_2\text{O}$ reagent. The surface of the spheres was folded and wrinkled, but in a different way as for $\text{Fe}(\text{NO}_3)_3 \cdot 9\text{H}_2\text{O}$: it seemed like the surface had sintered/fused together partly losing its microstructure.

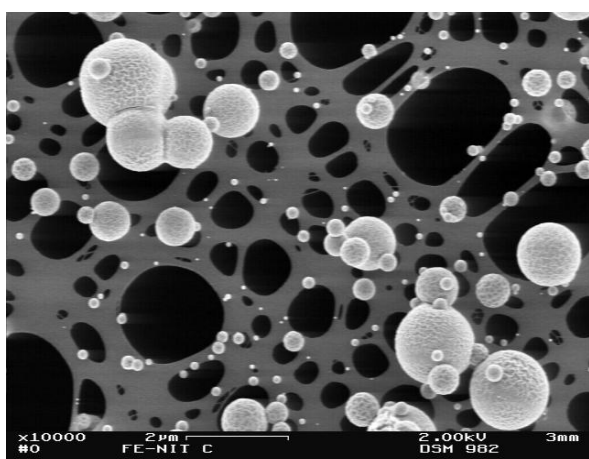


Fig. 13a. The generated particles with $\text{Fe}(\text{NO}_3)_3 \cdot 9\text{H}_2\text{O}$ reagent for continuous production (3.11.2010, no collection device). Particles are different sized spheres.

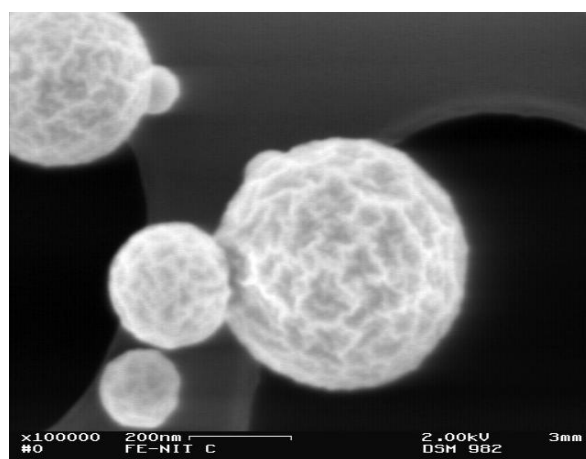


Fig. 13b. A detail of spherical particles. The surface of the particles is folded and wrinkled, and smallest particles are <200 nm in diameter.

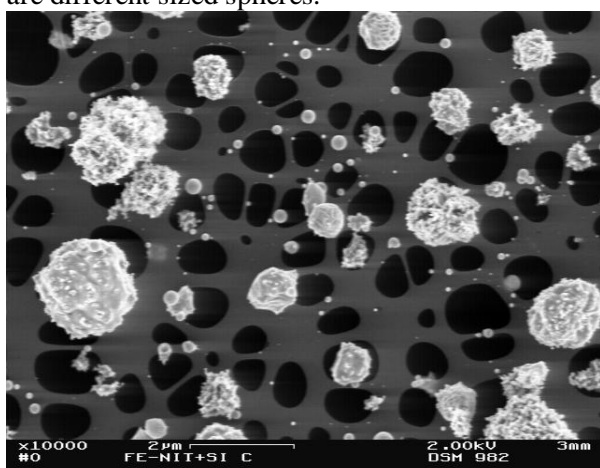


Fig. 14a. The generated particles with $\text{Fe}(\text{NO}_3)_3 \cdot 9\text{H}_2\text{O} + \text{silica}$ reagent for continuous production (4.11.2010, no collection device). The sphericity of particles has decreased, and the surface is not as smooth as without silica.

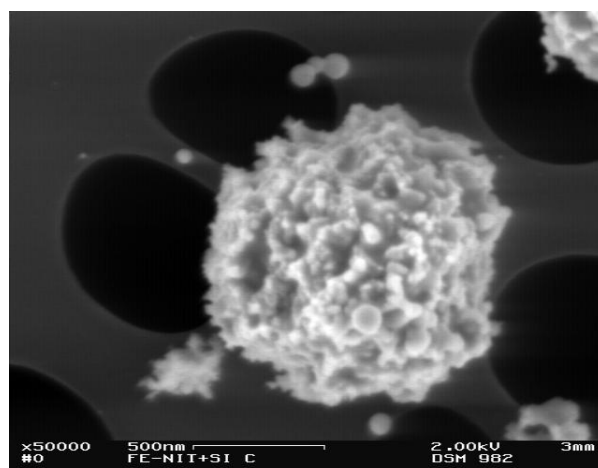


Fig. 14b. A detail of an almost spherical particle. There are very small spherical, primary particles (diameter approx. 20 nm) on the surface of a cobble-stone like structure.

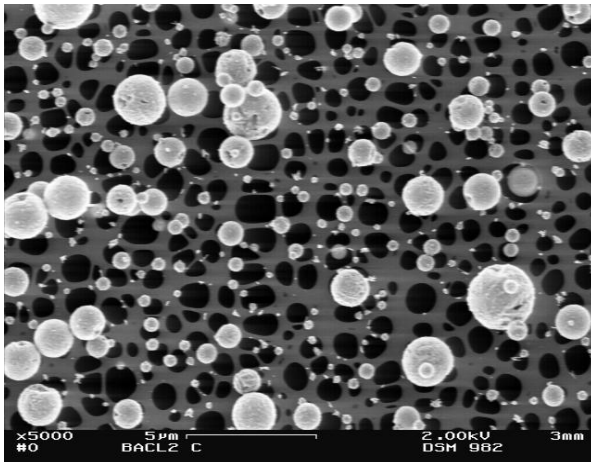


Fig. 15a. The generated particles with BaCl_2 reagent for continuous production (4.11.2010, no collection device). Particles are different sized spheres.

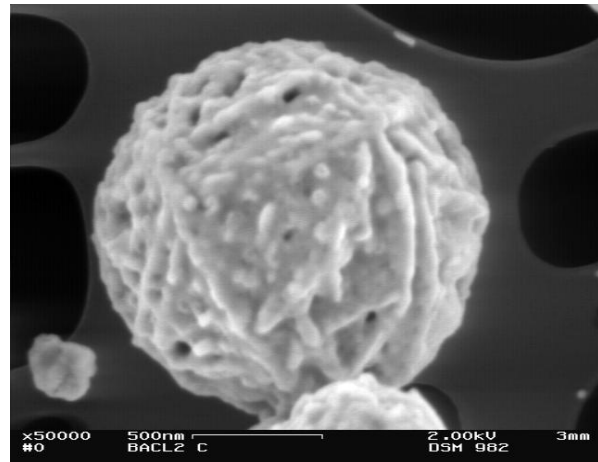


Fig. 15b. A detail of the collected particles. The surface of the particles is folded and wrinkled, but in a different way as for $\text{Fe}(\text{NO}_3)_3 \cdot 9\text{H}_2\text{O}$ (Fig. 13b).

3.2 Filter collection of produced particles

3.2.1 $\text{Fe}(\text{NO}_3)_3 \cdot 9\text{H}_2\text{O}$ and $\text{Fe}(\text{NO}_3)_3 \cdot 9\text{H}_2\text{O} + \text{Ba}(\text{NO}_3)_2$

3.2.1.1 Particle number concentration and number size distribution

Particle number concentration and size distribution was measured with an ELPI. Typical particle number concentration during the normal pulsed particle generation (collection of the particles by a new filter) with $\text{Fe}(\text{NO}_3)_3 \cdot 9\text{H}_2\text{O}$ reagent (40 g/dm^3 , 10 ml/min) varied between $2.0\text{--}2.1 \cdot 10^7$ $1/\text{cm}^3$ (Fig. 16). A test with powerful consecutive air “blows” (in this case 3) only was carried out to see how rapidly the number concentration of the particles decreases when no particles are collected on the filter. The number concentration during the first blow was approximately $1.7 \cdot 10^7$ $1/\text{cm}^3$, and during the third “blow” $7.0 \cdot 10^6$ $1/\text{cm}^3$, i.e. less than half of that during the “blows” with particle collection. The aerodynamic count median diameter (CMD_{ae}) of the particles varied approximately between 1–2 μm , and the “blow” with or without particle collection had no significant effect on the particle CMD_{ae} (Fig. 16).

With $\text{Fe}(\text{NO}_3)_3 \cdot 9\text{H}_2\text{O} + \text{Ba}(\text{NO}_3)_2$ (40 g/dm^3 , 15 + 4 ml/min) reagent the typical particle number concentration during the normal pulsed particle generation (collection of the particles by a new filter) varied between $1.6\text{--}1.7 \cdot 10^7$ $1/\text{cm}^3$ (Fig. 16). A similar test with powerful consecutive air “blows” (in this case 2) only indicated that the number concentration of the particles decreased down to $1.5 \cdot 10^7$ $1/\text{cm}^3$, i.e. basically no decrease in number concentration was found. It should be noted that the filter element was not changed between the collection of particles generated by different reagents. Thus the filter element was, at least partially “saturated” with particles and, therefore the particle number concentration during later “blows” without any particle collection maybe higher than they would be with a clean filter. The aerodynamic count median diameter (CMD_{ae}) of the particles var-

ied approximately between 1-2 μm for “blows” with particle collection. For “blows” without particle collection the CMD_{ae} of the particles was clearly smaller varying between 0.1-0.4 μm (Fig. 16).

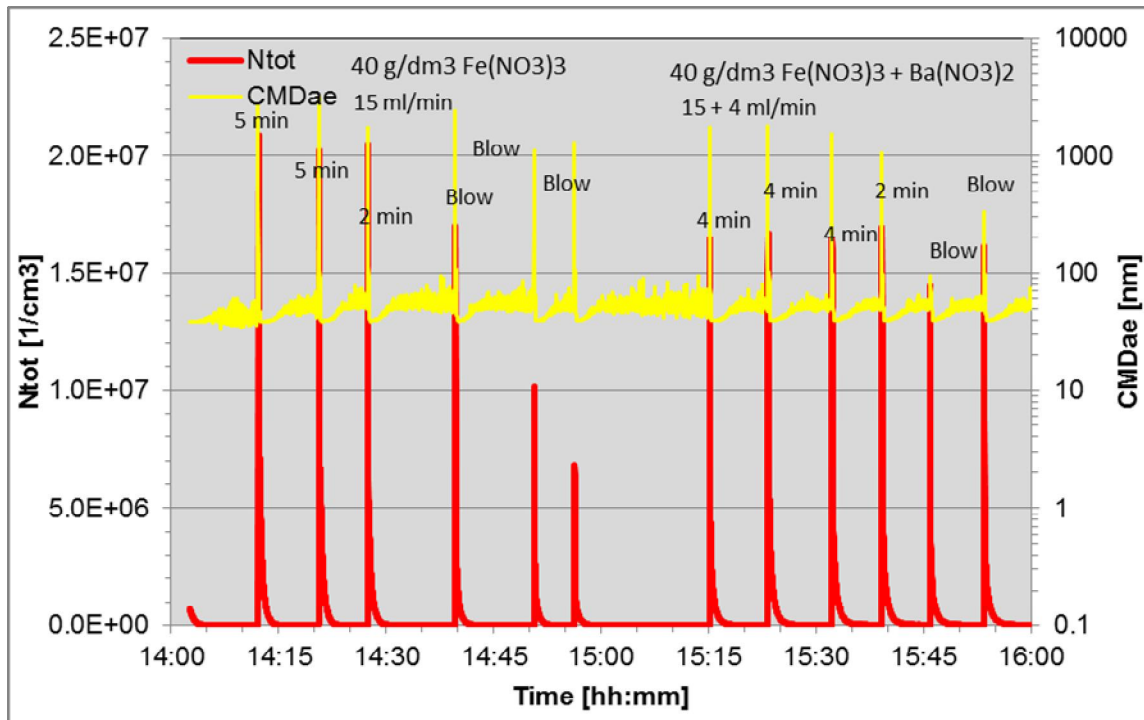


Fig. 16. Total particle number concentration and aerodynamic count median diameter (CMD_{ae}) of the particles generated from $\text{Fe}(\text{NO}_3)_3 \cdot 9\text{H}_2\text{O}$ and $\text{Fe}(\text{NO}_3)_3 \cdot 9\text{H}_2\text{O} + \text{Ba}(\text{NO}_3)_2$ reagent measured with ELPI on **30.8. 2011**. The particles are collected (collection time indicates as min) on a filter, and pulses generated by a powerful “blow” of air (10 bar) through the filter. “Blow” indicates “blowing” air through the filter without any collection of the particles.

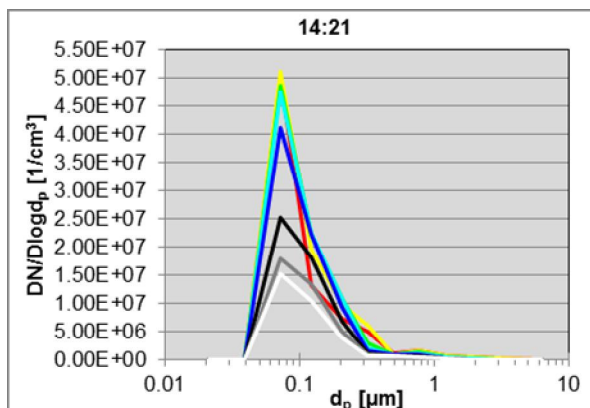


Fig. 17a. The evolution of the number size distribution during one charge (pulse) at 14:21 (Fig. 16), reagent $\text{Fe}(\text{NO}_3)_3 \cdot 9\text{H}_2\text{O}$.

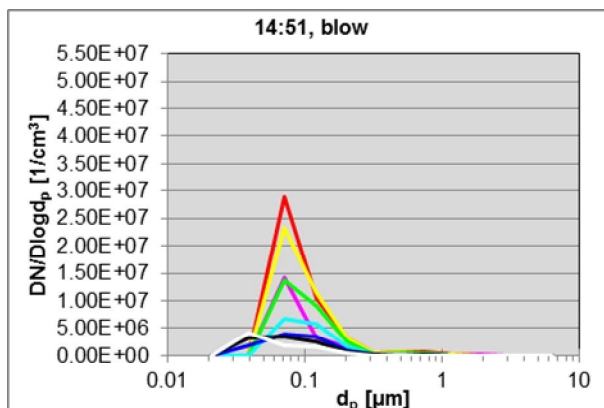


Fig. 17b. The evolution of the number size distribution during one charge (pulse) at 14:51 (Fig. 16), reagent $\text{Fe}(\text{NO}_3)_3 \cdot 9\text{H}_2\text{O}$, no particle collection.

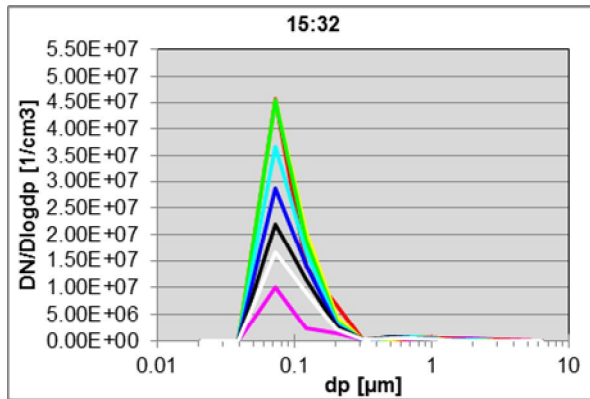


Fig. 17c. The evolution of the number size distribution during one charge (pulse) at 15:32 (Fig. 16), reagent $\text{Fe}(\text{NO}_3)_3 \cdot 9\text{H}_2\text{O} + \text{Ba}(\text{NO}_3)_2$.

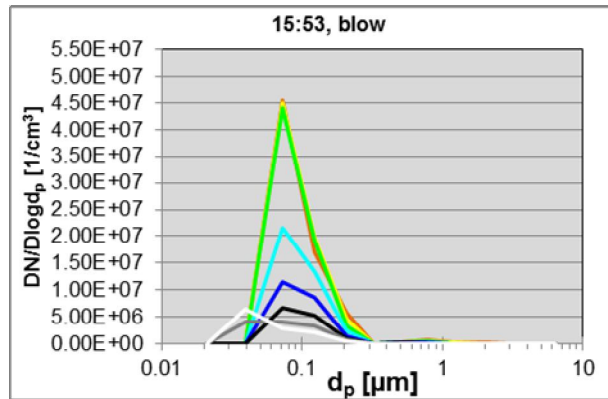


Fig. 17d. The evolution of the number size distribution during one charge (pulse) at 15:53 (Fig. 16), reagent $\text{Fe}(\text{NO}_3)_3 \cdot 9\text{H}_2\text{O} + \text{Ba}(\text{NO}_3)_2$, no particle collection

The number size distribution (NSD) with $\text{Fe}(\text{NO}_3)_3 \cdot 9\text{H}_2\text{O}$ reagent during one single pulse with filter collection of the particles was typically unimodal with a peak at approx. 70 nm (Fig. 17a). During “blow” without particle collection the location of the mode did not change (Fig. 17b). For $\text{Fe}(\text{NO}_3)_3 \cdot 9\text{H}_2\text{O} + \text{Ba}(\text{NO}_3)_2$ reagent the number size distribution (NSD) was also typically unimodal with a peak at approx. 80 nm (Fig. 17c). As with $\text{Fe}(\text{NO}_3)_3 \cdot 9\text{H}_2\text{O}$ reagent the location of the mode did not change during “blow” without particle collection (Fig. 17d).

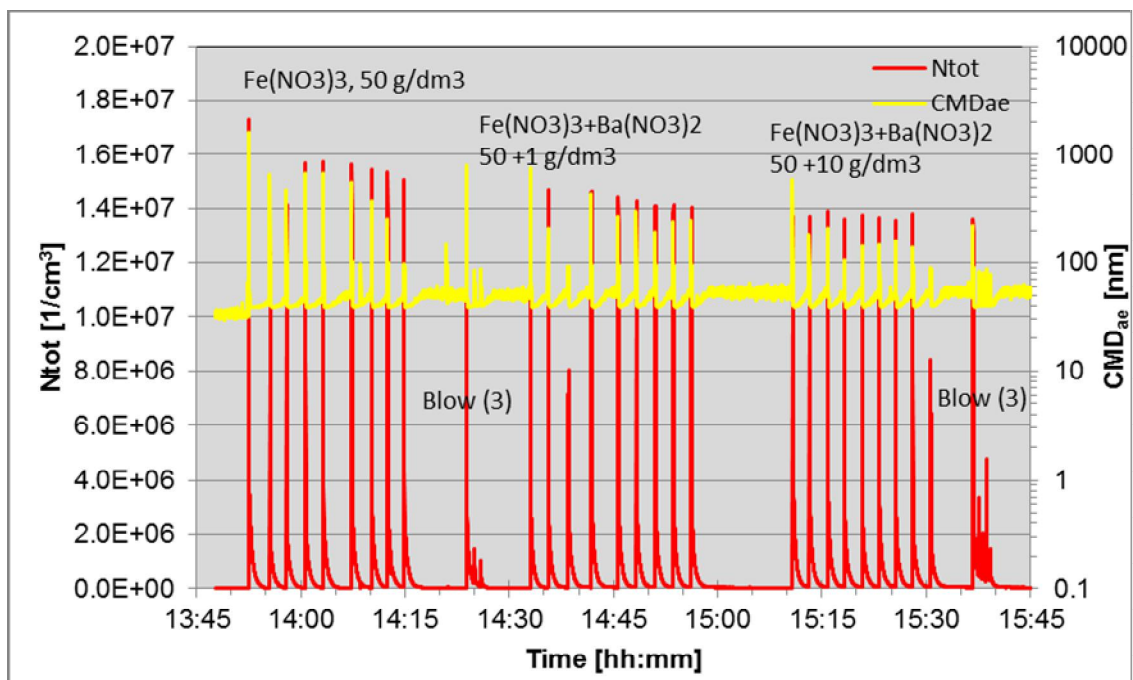


Fig. 18. Total particle number concentration and aerodynamic count median diameter (CMD_{ae}) of the particles generated from $\text{Fe}(\text{NO}_3)_3 \cdot 9\text{H}_2\text{O}$ and $\text{Fe}(\text{NO}_3)_3 \cdot 9\text{H}_2\text{O} + \text{Ba}(\text{NO}_3)_2$ reagent measured with ELPI on **31.8. 2011**. The particles are collected (collection time 1 min 20 s) on a filter, and pulses generated by a powerful “blow” of air (10 bar) through the filter. “Blow” indicates “blowing” air through the filter without any collection of the particles.

Typical particle number concentration during the normal pulsed particle generation (collection of the particles by a new filter) with $\text{Fe}(\text{NO}_3)_3 \cdot 9\text{H}_2\text{O}$ reagent (50 g/dm^3) varied between $1.4\text{--}1.7 \cdot 10^7 \text{ 1/cm}^3$ (Fig. 18). During the first “blow” with-

out particle collection the number concentration decreased to approximately $1.1 \cdot 10^7$ $1/\text{cm}^3$, and with consecutive “blows” down to approximately 1/10 of that of the “blows” with particle collection. There was quite large variation in the aerodynamic count median diameter (CMD_{ae}) of the particles: approximately from $0.1 \mu\text{m}$ to $2 \mu\text{m}$ (Fig. 18).

With $\text{Fe}(\text{NO}_3)_3 \cdot 9\text{H}_2\text{O} + \text{Ba}(\text{NO}_3)_2$ ($50 + 1 \text{ g}/\text{dm}^3$) reagent the typical particle number concentration during the normal pulsed particle generation (collection of the particles by a new filter) varied between $0.8\text{--}1.5 \cdot 10^7$ $1/\text{cm}^3$ (Fig. 18). The one pulse at approximately 14:38 was clearly lower than others: the reason for this is unclear. The aerodynamic count median diameter (CMD_{ae}) of the particles varied approximately between $0.2\text{--}0.8 \mu\text{m}$. Increasing the concentration of $\text{Ba}(\text{NO}_3)_2$ to $10 \text{ g}/\text{dm}^3$ did not cause any significant changes in either number concentration or in aerodynamic count median diameter (CMD_{ae}) of the particles (Fig. 18).

The number size distribution (NSD) with $\text{Fe}(\text{NO}_3)_3 \cdot 9\text{H}_2\text{O}$ reagent ($50 \text{ g}/\text{dm}^3$, $10 \text{ ml}/\text{min}$) during one single pulse with filter collection of the particles was typically unimodal with a peak at approx. 70 nm at the beginning of the “blow”. Towards the end of the “blow” the mode widened, and finally shifted towards smaller particles at approximately 40 nm (Fig. 19a). Addition of $\text{Ba}(\text{NO}_3)_2$ either $1 \text{ g}/\text{dm}^3$ or $10 \text{ g}/\text{dm}^3$ had no significant effect on the location of the mode of the particles in the number size distribution (Fig. 19b and 19c).

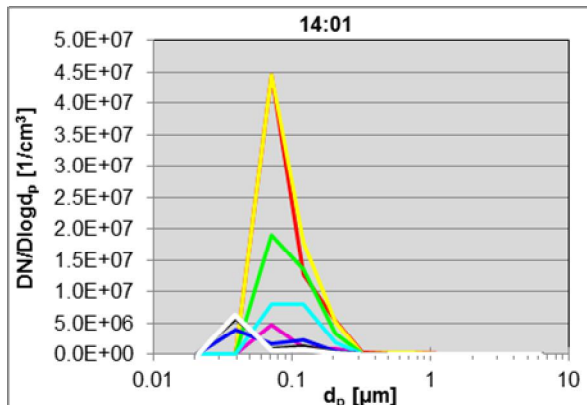


Fig. 19a. The evolution of the number size distribution during one charge (pulse) at 14:01 (Fig. 18), reagent $\text{Fe}(\text{NO}_3)_3 \cdot 9\text{H}_2\text{O}$.

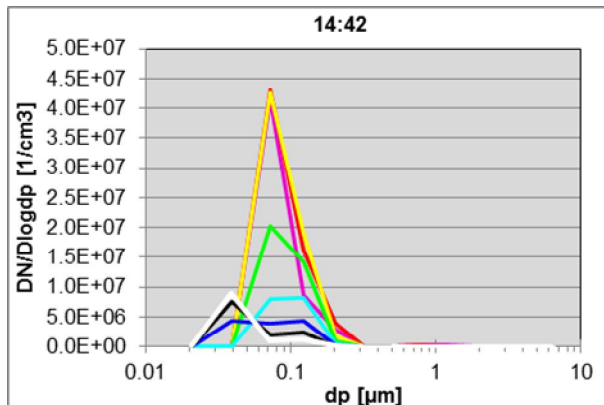


Fig. 19b. The evolution of the number size distribution during one charge (pulse) at 14:42 (Fig. 18), reagent $\text{Fe}(\text{NO}_3)_3 \cdot 9\text{H}_2\text{O} + \text{Ba}(\text{NO}_3)_2$.

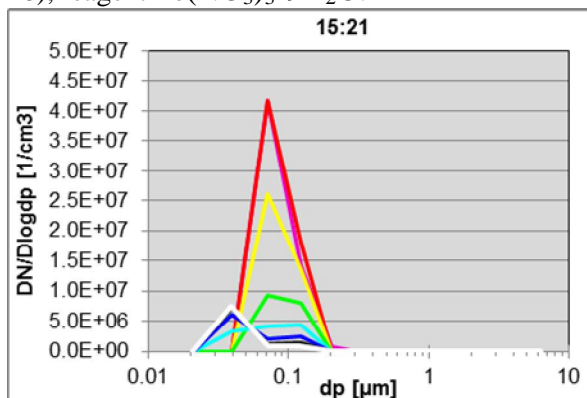


Fig. 19c. The evolution of the number size distribution during one charge (pulse) at 15:21 (Fig. 18), reagent $\text{Fe}(\text{NO}_3)_3 \cdot 9\text{H}_2\text{O} + \text{Ba}(\text{NO}_3)_2$.

3.2.1.2 Particle mass concentration and mass size distribution

Particle mass concentration was measured with a TEOM. Typical particle mass concentration during the normal pulsed particle generation (collection of the particles by a new filter) with $\text{Fe}(\text{NO}_3)_3 \cdot 9\text{H}_2\text{O}$ reagent (40 g/dm^3 , 15 ml/min) varied between $90\text{--}220 \text{ mg/m}^3$ (Fig. 20a). The lower mass concentration during the first “blow” was probably caused by the filter being clean, i.e. it had not “saturated” and thus some part of the particle mass was trapped in the pores of the filter. During “blows” without any particle collection the mass concentration varied between $30\text{--}70 \text{ mg/m}^3$ (Fig. 20a).

For $\text{Fe}(\text{NO}_3)_3 \cdot 9\text{H}_2\text{O} + \text{Ba}(\text{NO}_3)_2$ (40 g/dm^3 , $15 + 4 \text{ ml/min}$) reagent the typical particle mass concentration during the normal pulsed particle generation (collection of the particles by a new filter) varied between $80\text{--}100 \text{ mg/m}^3$. During “blows” without any particle collection the mass concentration was approximately 30 mg/m^3 (Fig. 20a).

For $\text{Fe}(\text{NO}_3)_3 \cdot 9\text{H}_2\text{O}$ reagent (50 g/dm^3 , 10 ml/min) the typical particle mass concentration during the normal pulsed particle generation (collection of the particles by a new filter) varied between $30\text{--}110 \text{ mg/m}^3$. The reason for the clearly higher first pulse was unclear. The mass concentration measured with a BLPI was 10.8 mg/m^3 (Fig. 21). The difference in measured mass concentration may have something to do with the chemical nature of the particles, because in some cases the consistency of the results between BLPI and TEOM are good and sometimes less good. This was also found here with using different reagents. During “blows” without any particle collection the mass concentration was approximately 35 mg/m^3 (Fig. 20a).

Addition of $\text{Ba}(\text{NO}_3)_2$ from 1 or 10 g/dm^3 did not cause any significant differences in mass concentration compared to the case without any $\text{Ba}(\text{NO}_3)_2$: with 1 g/dm^3 the mass concentration varied between $20\text{--}30 \text{ mg/m}^3$ (BLPI 10.3 mg/m^3 , Fig 21) and with 10 g/dm^3 between $20\text{--}40 \text{ mg/m}^3$ (Fig. 20b; BLPI 11.9 mg/m^3 , Fig. 21). The difference in measured mass concentration may have something to do with the chemical nature of the particles, because in some cases the consistency of the results between BLPI and TEOM are good and sometimes less good. This was also found here with using different reagents.

The much lower total particle mass concentration in the case of experiments on 30.8.2011 (Fig. 20a) compared to 31.8.2011 (Fig. 20b) was afterwards traced to the different filter used in these experiments. The filter used in experiments on 31.8.2011 (Fig. 20b) must have been of different material, because it was found to have a much worse collection efficiency than the one used on 30.8.2011: a significant part of the collected particles were able to penetrate through the filter material.

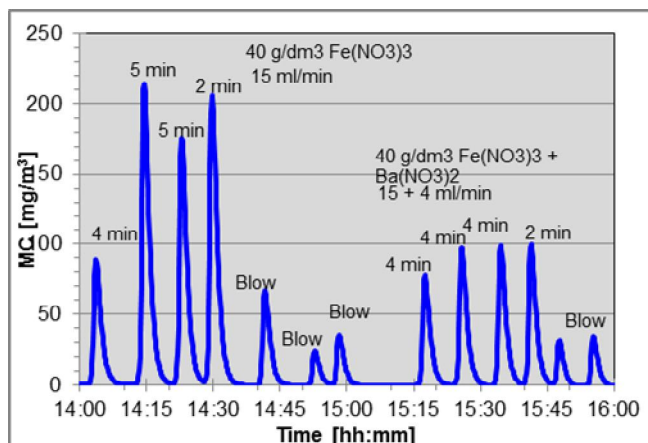


Fig. 20a. Mass concentration of the particles generated from $\text{Fe}(\text{NO}_3)_3 \cdot 9\text{H}_2\text{O}$ reagent measured with a TEOM (See Fig. 16 and 17).

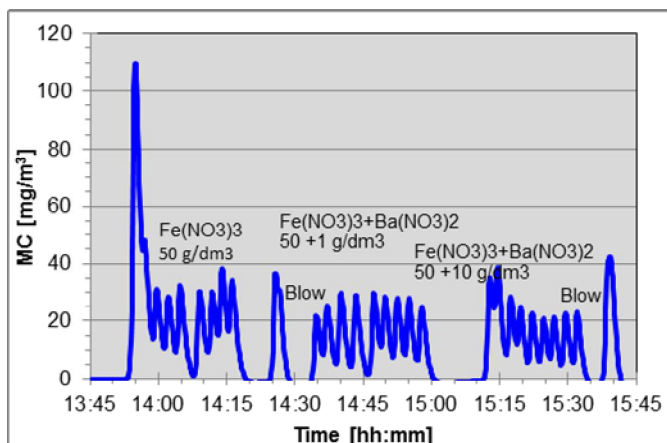


Fig. 20b. Mass concentration of the particles generated from $\text{Fe}(\text{NO}_3)_3 \cdot 9\text{H}_2\text{O} + \text{Ba}(\text{NO}_3)_2$ reagent measured with a TEOM (See Fig. 18 and 19).

The mass size distribution for the normal pulsed particle generation (collection of the particles by a new filter) with $\text{Fe}(\text{NO}_3)_3 \cdot 9\text{H}_2\text{O}$ and $\text{Fe}(\text{NO}_3)_3 \cdot 9\text{H}_2\text{O} + \text{Ba}(\text{NO}_3)_2$ reagent were clearly bimodal, and almost identical independent on the addition of $\text{Ba}(\text{NO}_3)_2$ reagent. The small particle mode was at approximately 70 nm, and “large” particle mode at approximately 6 μm (assuming unit density of the particles, Fig. 21). For comparison, a mass size distributions from previous experiment (11/2010) for $\text{Fe}(\text{NO}_3)_3 \cdot 9\text{H}_2\text{O}$ and $\text{Fe}(\text{NO}_3)_3 \cdot 9\text{H}_2\text{O} + \text{silica}$ reagent with continuous production of particles (no collection device) had a small particle mode at the same location as the ones produced by normal pulsed particle generation (collection of the particles by a new filter). However, the large particle mode at 6 μm is missing. Thus it seems that the particles were agglomerating at the filter collection possibly because of the water condensation at the lower temperature than usual with the cyclone collection during the filter collection of the particles. It should be noted that, unfortunately, these BLPI measurements were carried out with the leaking filter.

Table 3. Particle fractions (%) under and over 1 μm (aerodynamic size) and corresponding total mass concentration measured with a BLPI (see. Fig. 21).

Reagent	< 1 μm [%]	> 1 μm [%]	C(tot) [mg/m^3]
$\text{Fe}(\text{NO}_3)_3 \cdot 9\text{H}_2\text{O}$ (50g/dm ³)	28	72	10.8
$\text{Fe}(\text{NO}_3)_3 \cdot 9\text{H}_2\text{O} +$ $\text{Ba}(\text{NO}_3)_2$ (50+1g/dm ³)	32	68	10.3
$\text{Fe}(\text{NO}_3)_3 \cdot 9\text{H}_2\text{O} +$ $\text{Ba}(\text{NO}_3)_2$ (40+10g/dm ³)	32	68	11.8
$\text{Fe}(\text{NO}_3)_3 \cdot 9\text{H}_2\text{O}$ contin- uous	57	43	7.0
$\text{Fe}(\text{NO}_3)_3 \cdot 9\text{H}_2\text{O} + \text{silica}$, continuous	74	26	9.4

Dividing the particles roughly into two particle fractions, under and over 1 μm (aerodynamic size, Table 3) it was found that during the continuous production of the particles (11/2010) nearly over 60 % of the mass of the particles was found in smaller than 1 μm sized particles. During the normal pulsed particle generation (collection of the particles by a new filter) only 30 % of the mass was found in

smaller than $1 \mu\text{m}$ sized particles. This also indicated that agglomeration at the filter collection possibly because of the water condensation at the lower temperature than usual with the cyclone collection occurred. However, there may also be other causes for agglomeration of the particles.

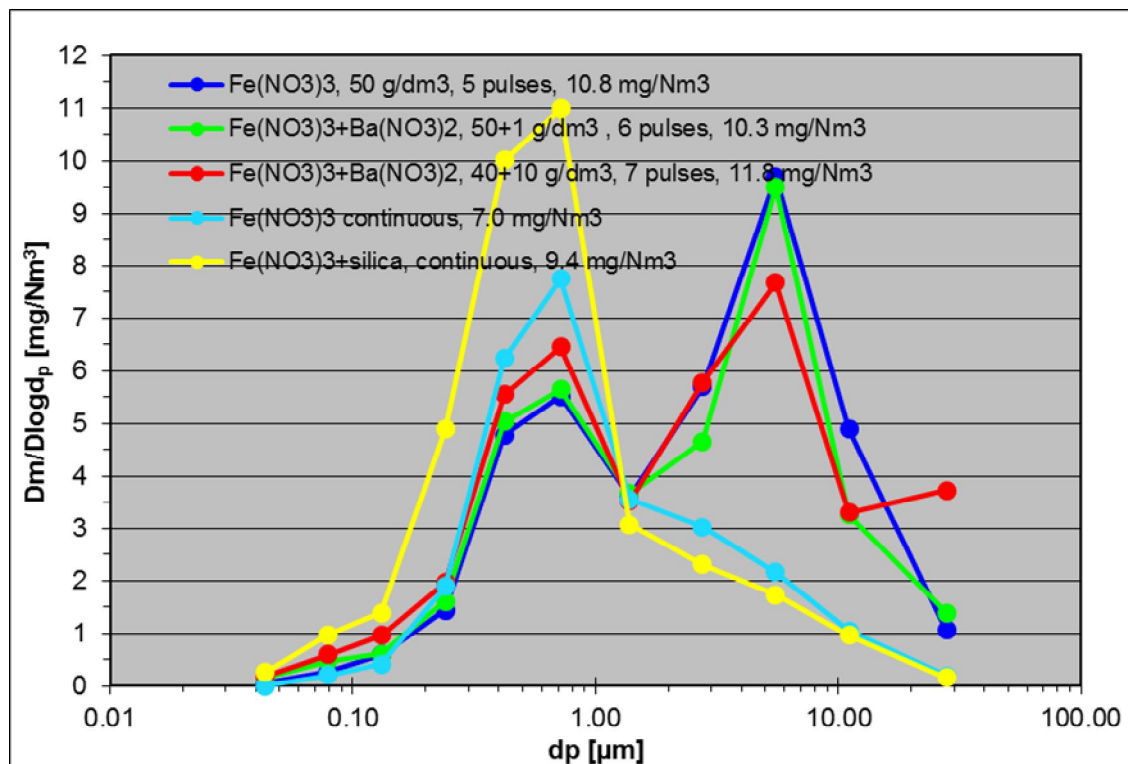


Fig. 21. Particle mass size distribution of the particles generated from $\text{Fe}(\text{NO}_3)_3 \cdot 9\text{H}_2\text{O}$ and $\text{Fe}(\text{NO}_3)_3 \cdot 9\text{H}_2\text{O} + \text{Ba}(\text{NO}_3)_2$ reagent measured with BLPI during campaign 09/2011 and collected on a filter followed by a “blow”. For comparison, $\text{Fe}(\text{NO}_3)_3 \cdot 9\text{H}_2\text{O}$ and $\text{Fe}(\text{NO}_3)_3 \cdot 9\text{H}_2\text{O} + \text{silica}$ mass size distribution with continuous production of particles (no collection device) from earlier measurements (11/2010; Fig. 12) has been added.

3.2.1.3 Particle morphology

The collecting filter element after the experiment on **30.8.2011** ($\text{Fe}(\text{NO}_3)_3 \cdot 9\text{H}_2\text{O}$ and $\text{Fe}(\text{NO}_3)_3 \cdot 9\text{H}_2\text{O} + \text{Ba}(\text{NO}_3)_2$ reagents, Fig. 22a and 22b) looked like condensation of possibly water vapour had occurred (the dark centre area on the filter). Indication of the possible water vapour condensation was also found at the backside of the filter element (Fig. 22b).

For **31.8.2011** ($\text{Fe}(\text{NO}_3)_3 \cdot 9\text{H}_2\text{O}$ and $\text{Fe}(\text{NO}_3)_3 \cdot 9\text{H}_2\text{O} + \text{Ba}(\text{NO}_3)_2$ reagents.) experiment with a new filter element it seemed that very small amount of the produced particles were collected on the collecting side of the filter (Fig. 22c). Looking at the backside of the same filter indicated serious leakage / particle penetration through the filter element: there were more particles on the backside than on the collecting side of the filter element (Fig. 22d). It should be noted that this element also looked visually different in colour than the other filters.

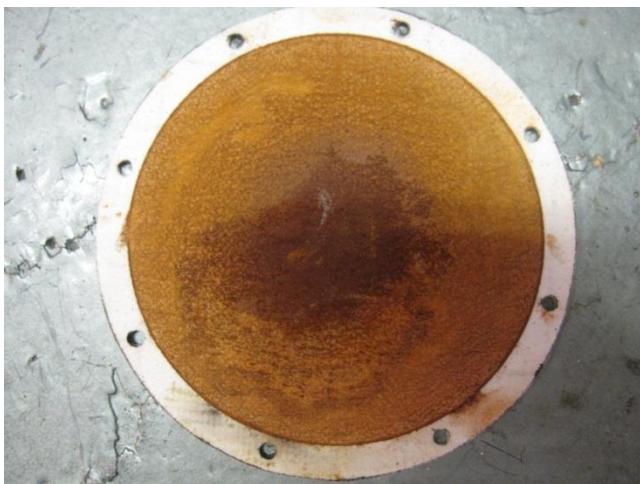


Fig. 22a. The collecting side of the filter after the experiment on **30.8.2011** used for collecting particles produced from $\text{Fe}(\text{NO}_3)_3 \cdot 9\text{H}_2\text{O}$ and $\text{Fe}(\text{NO}_3)_3 \cdot 9\text{H}_2\text{O} + \text{Ba}(\text{NO}_3)_2$ reagents.

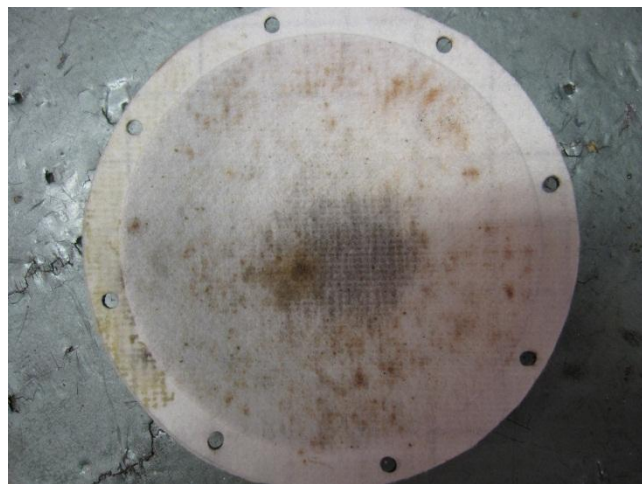


Fig. 22b. The non-collecting side of the filter after the experiment on **30.8.2011** used for collecting particles produced from $\text{Fe}(\text{NO}_3)_3 \cdot 9\text{H}_2\text{O}$ and $\text{Fe}(\text{NO}_3)_3 \cdot 9\text{H}_2\text{O} + \text{Ba}(\text{NO}_3)_2$ reagents.



Fig. 22c. The collecting side of the filter after the experiment on **31.8.2011** used for collecting particles produced from $\text{Fe}(\text{NO}_3)_3 \cdot 9\text{H}_2\text{O}$ and $\text{Fe}(\text{NO}_3)_3 \cdot 9\text{H}_2\text{O} + \text{Ba}(\text{NO}_3)_2$ reagents.

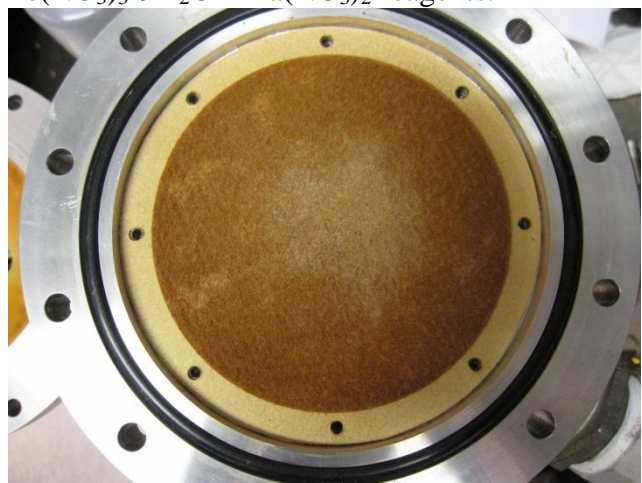


Fig. 22d. The non-collecting side of the filter after the experiment on **31.8.2011** used for collecting particles produced from $\text{Fe}(\text{NO}_3)_3 \cdot 9\text{H}_2\text{O}$ and $\text{Fe}(\text{NO}_3)_3 \cdot 9\text{H}_2\text{O} + \text{Ba}(\text{NO}_3)_2$ reagents.

The individual particle samples were collected with an aspiration electron microscopy sampler (AEM sampler). With the $\text{Fe}(\text{NO}_3)_3 \cdot 9\text{H}_2\text{O}$ 30.8.2011 reagent during normal pulsed generation the particles (collection with a new filter) majority of the particles were no longer single spheres (though single spheres were still found) as in the case of continuous production of particles (no collection device) but a different sized aggregates up to about $2 \mu\text{m}$ in size (Fig 23a and 23b). Adding $\text{Ba}(\text{NO}_3)_2$ caused the particles to form even more aggregates, though the actual particle size did not seem to change significantly (23c and 23d).

For 31.8.2011 the interpretation of the results may be affected by the leaking filter element, because some of the produced particles were able to penetrate the filter and were not collected. For $\text{Fe}(\text{NO}_3)_3 \cdot 9\text{H}_2\text{O}$ (50 g/dm^3) it would seem that no significant difference to the case with $40 \text{ g/dm}^3 \text{ Fe}(\text{NO}_3)_3 \cdot 9\text{H}_2\text{O}$ was found (Fig. 24a and 24b). Adding $\text{Ba}(\text{NO}_3)_2$ either 1 or 10 g/dm^3 seemed to cause the particles to form even more aggregates, though the actual particle size did not seem to change significantly (24c-24f). It should be, though, noted that these results were obtained using a leaking filter.

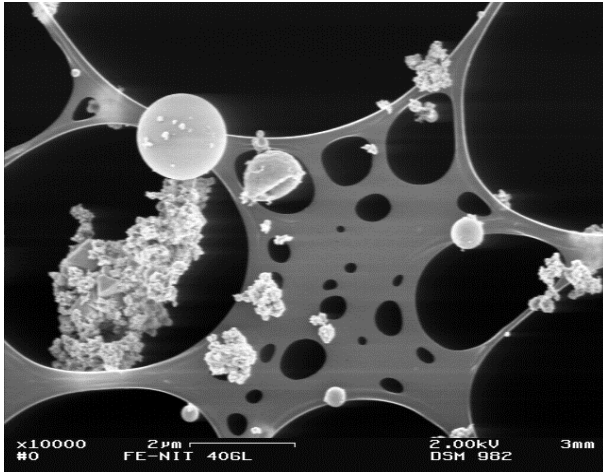


Fig. 23a. The generated particles with $\text{Fe}(\text{NO}_3)_3 \cdot 9\text{H}_2\text{O}$ reagent (30.8.2011) collected with a filter and “blown” away. Particles are, generally smaller than $2 \mu\text{m}$.

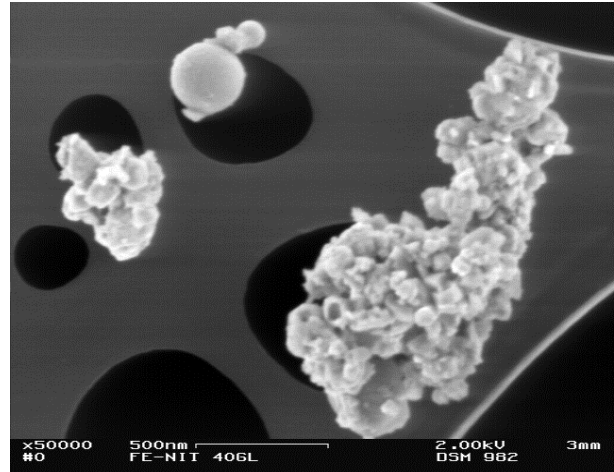


Fig. 23b. A detailed image of the particles. Particles are no longer only single spheres, also agglomerates were found.

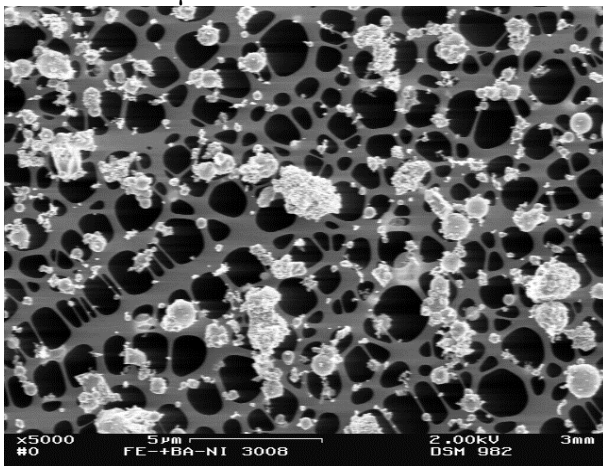


Fig. 23c. The generated particles with $\text{Fe}(\text{NO}_3)_3 \cdot 9\text{H}_2\text{O} + \text{Ba}(\text{NO}_3)_2$ reagent (30.8.2011) collected with a filter and “blown” away.

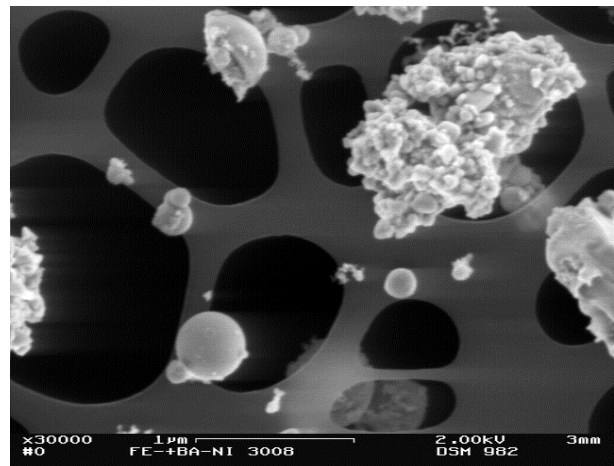


Fig. 23d. A detailed image of the particles. Structure of the particles is almost identical to those without the addition of $\text{Ba}(\text{NO}_3)_2$.

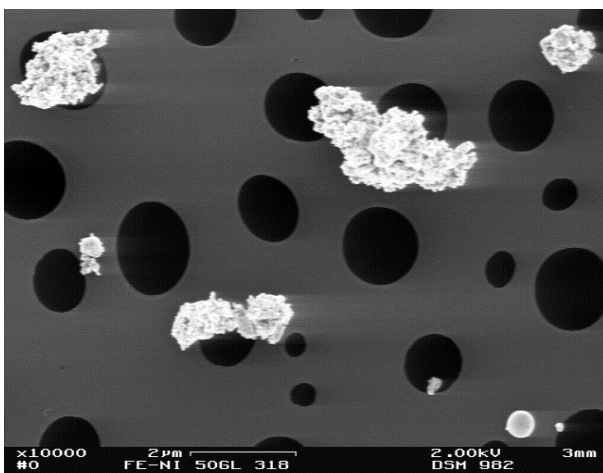


Fig. 24a. The generated particles with $\text{Fe}(\text{NO}_3)_3 \cdot 9\text{H}_2\text{O}$ (50 g/dm^3) reagent (31.8.2011) collected with a filter and “blown” away. Particles are, generally smaller than $2 \mu\text{m}$.

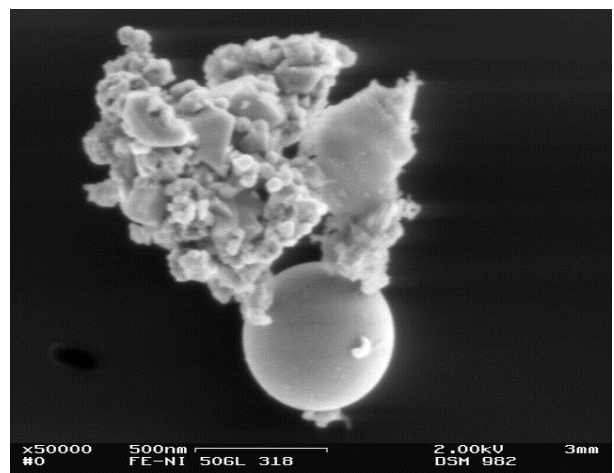


Fig. 24b. A detailed image of the particles. Agglomerates consisted of very different structures: different sized spheres, irregular shaped particles.

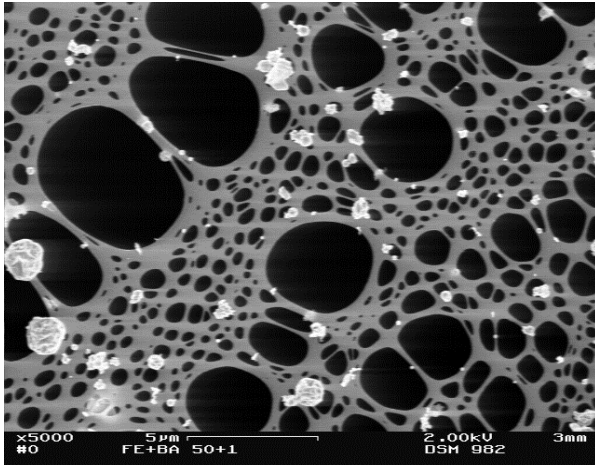


Fig. 24c. The generated particles with $\text{Fe}(\text{NO}_3)_3 \cdot 9\text{H}_2\text{O} + \text{Ba}(\text{NO}_3)_2$ (50+1 g/dm^3) reagent (31.8.2011) collected with a filter and “blown” away.

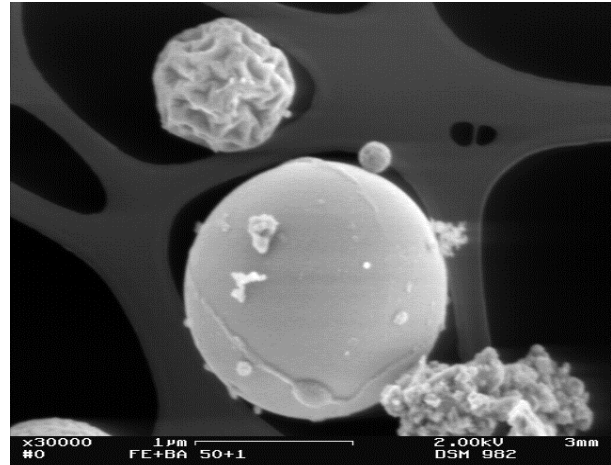


Fig. 24d. A detailed image of the particles. Different sized spheres and agglomerates were found.

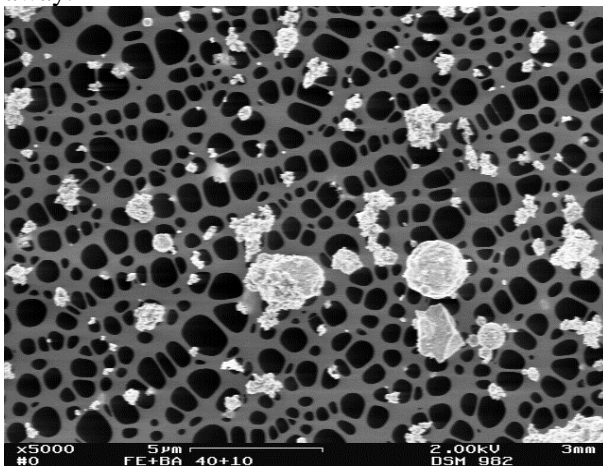


Fig. 24e. The generated particles with $\text{Fe}(\text{NO}_3)_3 \cdot 9\text{H}_2\text{O} + \text{Ba}(\text{NO}_3)_2$ (40+10 g/dm^3) reagent (31.8.2011) collected with a filter and “blown” away.

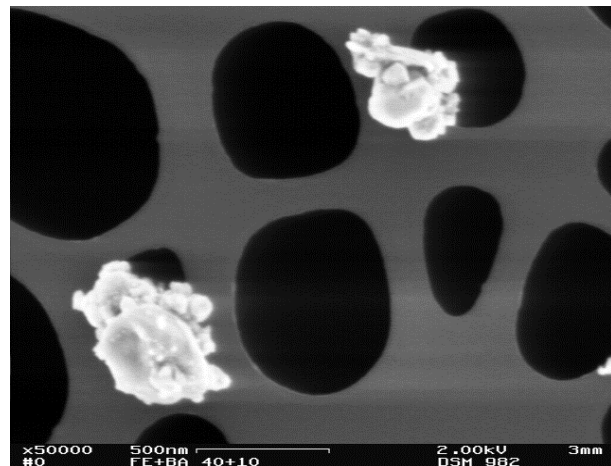


Fig. 24f. A detailed image of the particles. Majority of the particles seemed to be agglomerates

3.2.2 $\text{Ba}(\text{NO}_3)_2$, BaCl_2 , $\text{Ba}(\text{NO}_3)_2 + \text{Al}(\text{NO}_3)_3$ and $\text{Fe}(\text{NO}_3)_3 \cdot 9\text{H}_2\text{O} + \text{NaNO}_3$

3.2.2.1 Particle number concentration and number size distribution

Particle number concentration and size distribution was measured with an ELPI. Typical particle number concentration during the normal pulsed particle generation (collection of the particles by a new filter) with $\text{Ba}(\text{NO}_3)_2$ reagent (50 g/dm^3) varied between $1.0\text{--}1.8 \cdot 10^7$ $1/\text{cm}^3$. A test with powerful consecutive air “blows” (in this case only 1) only the number concentration decreased to approximately $3.0 \cdot 10^6$ $1/\text{cm}^3$. The aerodynamic count median diameter (CMD_{ae}) of the particles varied approximately between 1.8–2.5 μm , and the “blow” with or without particle collection had no significant effect on the particle CMD_{ae} (Fig. 25).

With BaCl_2 (50 g/dm^3) reagent the particle number concentration during the normal pulsed particle generation (collection of the particles by a new filter) varied

between $1.3\text{-}1.5 \cdot 10^7$ $1/\text{cm}^3$. For consecutive air “blows” (in this case 2) only the number concentration decreased down to approximately $3.0 \cdot 10^6$ $1/\text{cm}^3$. The aerodynamic count median diameter (CMD_{ae}) of the particles varied approximately between $1.8\text{-}2.5$ μm for “blows” with particle collection, and for “blows” without particle collection between $1.2\text{-}1.9$ μm (Fig. 25).

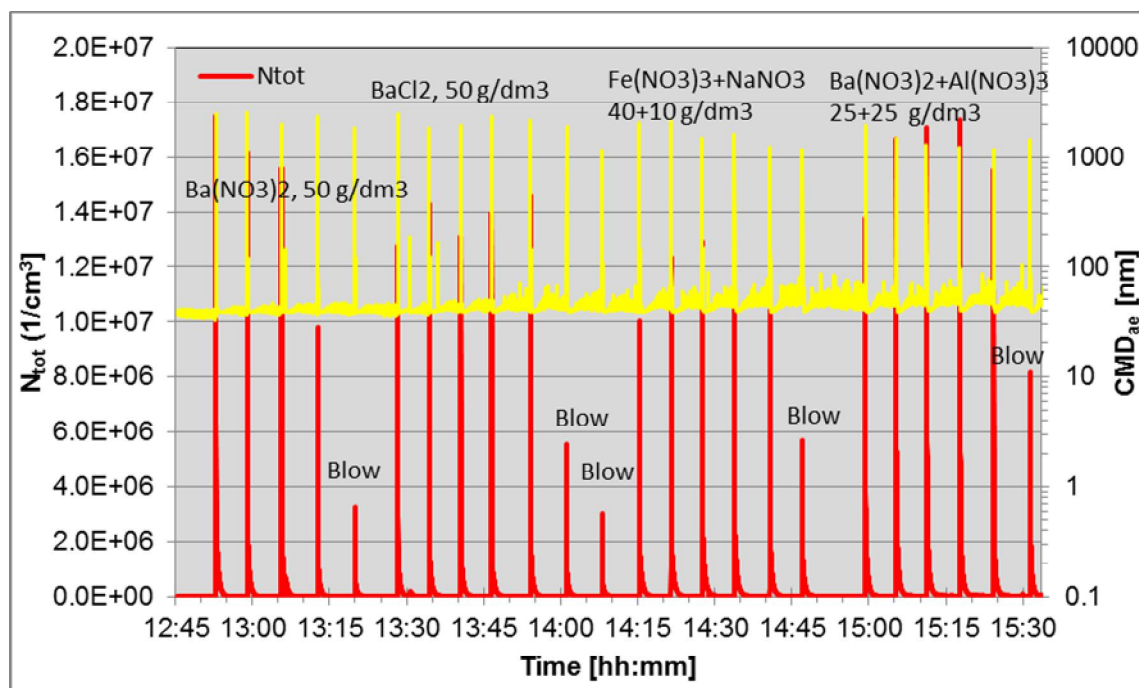


Fig. 25. Total particle number concentration and aerodynamic count median diameter (CMD_{ae}) of the particles generated from $\text{Ba}(\text{NO}_3)_2$, BaCl_2 , $\text{Ba}(\text{NO}_3)_2 + \text{Al}(\text{NO}_3)_3$ and $\text{Fe}(\text{NO}_3)_3 \cdot 9\text{H}_2\text{O} + \text{NaNO}_3$ reagents measured with ELPI on **1.9. 2011**. The particles are collected (collection time 5 min) on a filter, and pulses generated by a powerful “blow” of air (10 bar) through the filter. “Blow” indicates “blowing” air through the filter without any collection of the particles.

For $\text{Fe}(\text{NO}_3)_3 \cdot 9\text{H}_2\text{O} + \text{NaNO}_3$ ($25+25$ g/dm^3) reagent the particle number concentration during the normal pulsed particle generation (collection of the particles by a new filter) varied between $1.0\text{-}1.3 \cdot 10^7$ $1/\text{cm}^3$. For consecutive air “blows” (in this case only 1) only the number concentration decreased to approximately $6.0 \cdot 10^6$ $1/\text{cm}^3$. The aerodynamic count median diameter (CMD_{ae}) of the particles varied approximately between $1.2\text{-}2.1$ μm , and the “blow” with or without particle collection had no significant effect on the particle CMD_{ae} (Fig. 25).

For $\text{Ba}(\text{NO}_3)_2 + \text{Al}(\text{NO}_3)_3$ ($25+25$ g/dm^3) reagent the particle number concentration during the normal pulsed particle generation (collection of the particles by a new filter) varied between $1.4\text{-}1.7 \cdot 10^7$ $1/\text{cm}^3$. For consecutive air “blows” (in this case only 1) only the number concentration decreased to approximately $8.0 \cdot 10^6$ $1/\text{cm}^3$. The aerodynamic count median diameter (CMD_{ae}) of the particles varied approximately between $1.2\text{-}2$ μm , and the “blow” with or without particle collection had no significant effect on the particle CMD_{ae} (Fig. 25). It can also be seen that the particle number concentration after “blows” without particle collection has an increasing trend as a function time: this also indicated the “saturation” of the filter. It should be noted, though, that only two “blows” at maximum was applied: if the number of “blows” had been higher, the “saturation degree” of the fil-

ter element would have probably been lower, as seen with two consecutive “blows”, e.g. for BaCl_2 (50 g/dm^3 , Fig. 25).

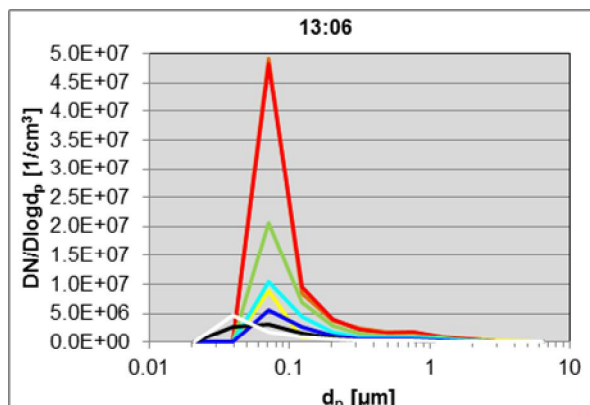


Fig. 26a. The evolution of the number size distribution during one charge (pulse) at 13:06 (Fig. 25), reagent $\text{Ba}(\text{NO}_3)_2$.

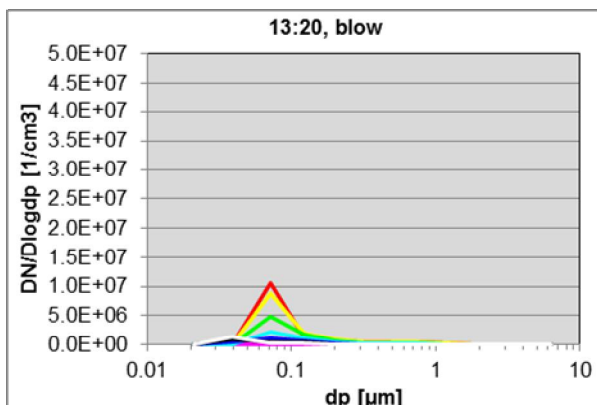


Fig. 26b. The evolution of the number size distribution during one charge (pulse) at 13:20 (Fig. 25), reagent $\text{Ba}(\text{NO}_3)_2$, no particle collection before.

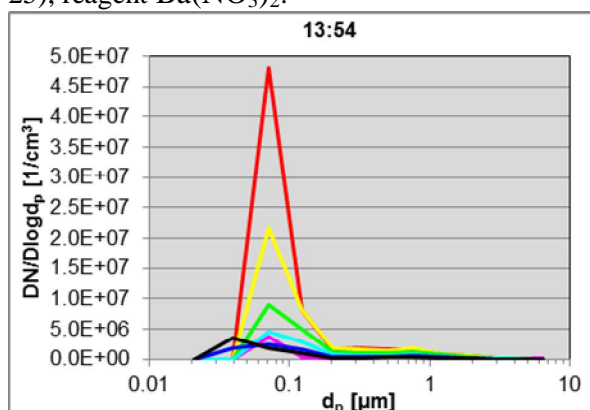


Fig. 26c. The evolution of the number size distribution during one charge (pulse) at 13:54 (Fig. 25), reagent BaCl_2 .

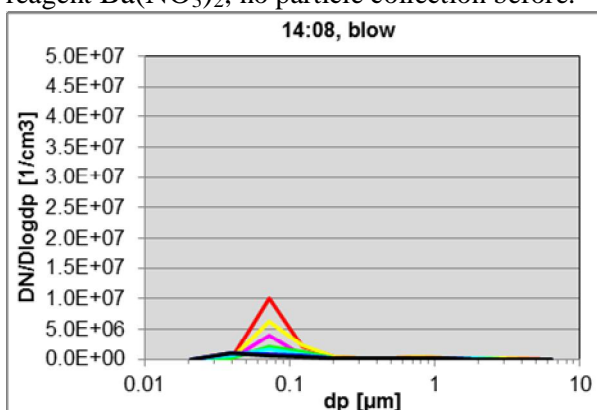


Fig. 26d. The evolution of the number size distribution during one charge (pulse) at 14:08 (Fig. 25), reagent BaCl_2 , no particle collection before.

The number size distribution (NSD) with $\text{Ba}(\text{NO}_3)_2$ reagent (50 g/dm^3) during one single pulse with filter collection of the particles was typically unimodal with a peak at approximately 80 nm at the beginning of the “blow”. Towards the end the end of the “blow” the mode widened, and finally shifted towards smaller particles at approximately 40 nm. A slight indication of the second mode at approximately 800 nm was also found (Fig. 26a). The “blow” without any particle collection had no significant effect on the mode of the number size distribution (Fig. 26b).

For BaCl_2 (50 g/dm^3) reagent during one single pulse with filter collection of the particles the number size distribution was typically unimodal with a peak at approximately 80 nm at the beginning of the “blow”. Similar behaviour as in the case for $\text{Ba}(\text{NO}_3)_2$ was found: towards the end the end of the “blow” the mode widened, and finally shifted towards smaller particles at approximately 40 nm. A slight indication of the second mode at approximately 800 nm was also found (Fig. 26c). The “blow” without any particle collection had no significant effect on the mode of the number size distribution as in the case for $\text{Ba}(\text{NO}_3)_2$ (Fig. 26d).

For $\text{Fe}(\text{NO}_3)_3 \cdot 9\text{H}_2\text{O} + \text{NaNO}_3$ ($25+25 \text{ g/dm}^3$) reagent during one single pulse with filter collection of the particles the number size distribution was typically unimodal with a peak at approximately 70 nm during entire “blow”. A slight indi-

cation of the second mode at approximately 200 nm was also found (Fig. 27a). The “blow” without any particle collection had no significant effect on the mode of the number size distribution (Fig. 27b).

For $\text{Ba}(\text{NO}_3)_2 + \text{Al}(\text{NO}_3)_3$ ($25+25 \text{ g/dm}^3$) reagent during one single pulse with filter collection of the particles the number size distribution was typically unimodal with a peak at approximately 80 nm at the beginning of the “blow”. Towards the end the end of the “blow” the mode shifted towards smaller particles at approximately 40 nm. A slight indication of the second mode at approximately 800 nm was also found (Fig. 28a). The “blow” without any particle collection had no significant effect on the mode of the number size distribution (Fig. 28b).

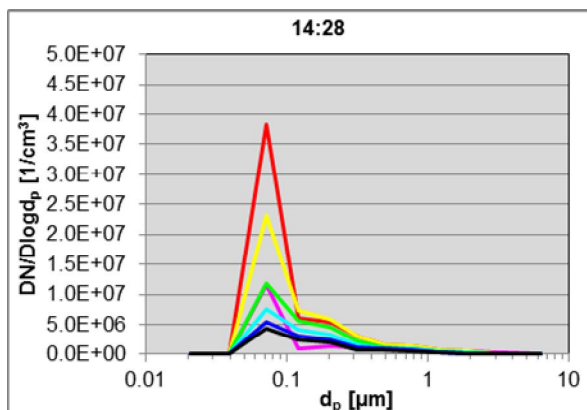


Fig. 27a. The evolution of the number size distribution during one charge (pulse) at 14:28 (Fig. 25), reagent $\text{Fe}(\text{NO}_3)_3 \cdot 9\text{H}_2\text{O} + \text{NaNO}_3$.

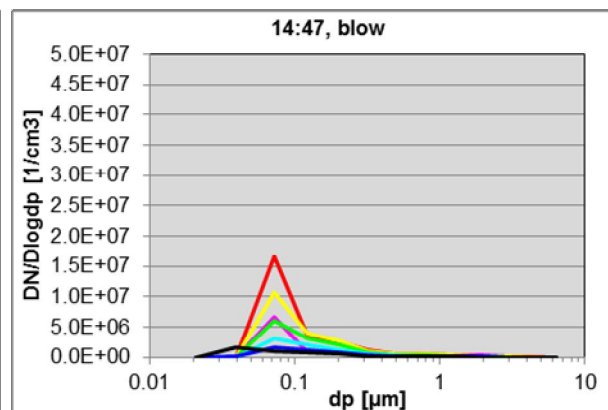


Fig. 27b. The evolution of the number size distribution during one charge (pulse) at 14:47 (Fig. 25), reagent $\text{Fe}(\text{NO}_3)_3 \cdot 9\text{H}_2\text{O} + \text{NaNO}_3$, no particle collection before.

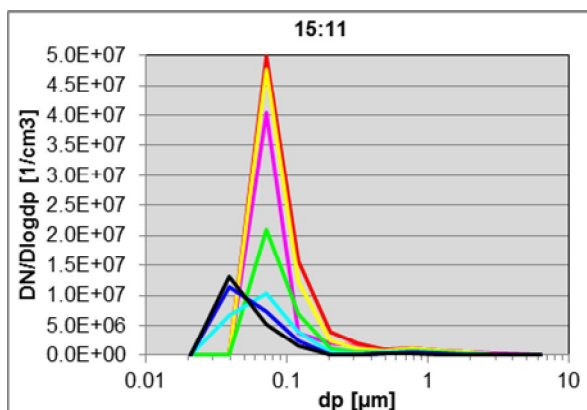


Fig. 28a. The evolution of the number size distribution during one charge (pulse) at 15:11 (Fig. 25), reagent $\text{Ba}(\text{NO}_3)_2 + \text{Al}(\text{NO}_3)_3$.

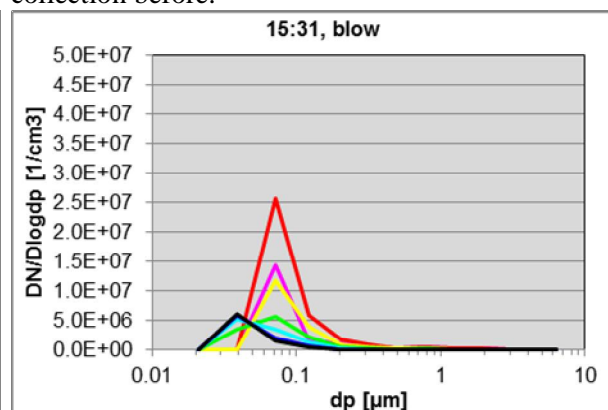


Fig. 28b. The evolution of the number size distribution during one charge (pulse) at 15:53 (Fig. 25), reagent $\text{Ba}(\text{NO}_3)_2 + \text{Al}(\text{NO}_3)_3$, no particle collection before.

3.2.2.2 Particle mass concentration

Particle mass concentration was measured with a TEOM. Typical particle mass concentration during the normal pulsed particle generation (collection of the particles by a new filter) with $\text{Ba}(\text{NO}_3)_2$ reagent (50 g/dm^3) varied between $140\text{-}200 \text{ mg/m}^3$. During “blows” without any particle collection the mass concentration varied between $20\text{-}100 \text{ mg/m}^3$ (Fig. 29).

With BaCl_2 (50 g/dm^3) reagent the particle mass concentration during the normal pulsed particle generation (collection of the particles by a new filter) with varied between $190\text{-}240 \text{ mg/m}^3$. During “blows” without any particle collection the mass concentration varied between $30\text{-}70 \text{ mg/m}^3$ (Fig. 29).

For $\text{Fe}(\text{NO}_3)_3 \cdot 9\text{H}_2\text{O} + \text{NaNO}_3$ ($25+25 \text{ g/dm}^3$) reagent the particle mass concentration during the normal pulsed particle generation (collection of the particles by a new filter) with varied between $150\text{-}270 \text{ mg/m}^3$. During “blows” (in this case only 1) without any particle collection the mass concentration decreased to 50 mg/m^3 (Fig. 29).

For $\text{Ba}(\text{NO}_3)_2 + \text{Al}(\text{NO}_3)_3$ ($25+25 \text{ g/dm}^3$) reagent the particle mass concentration during the normal pulsed particle generation (collection of the particles by a new filter) with varied between $130\text{-}280 \text{ mg/m}^3$. During “blows” (in this case only 1) without any particle collection the mass concentration decreased to 110 mg/m^3 (Fig. 29).

The trend of increasing mass concentration after “blows” towards the end of the experiment may be an indication of the “saturation” of the filter element: the pores of the filter element are full of particles, and they are deposited on the surface of the existing particles / filter material. The increased mass concentration may though, be a consequence of different reagents, too. The possible mutual effect of these cannot, however, be distinguished.

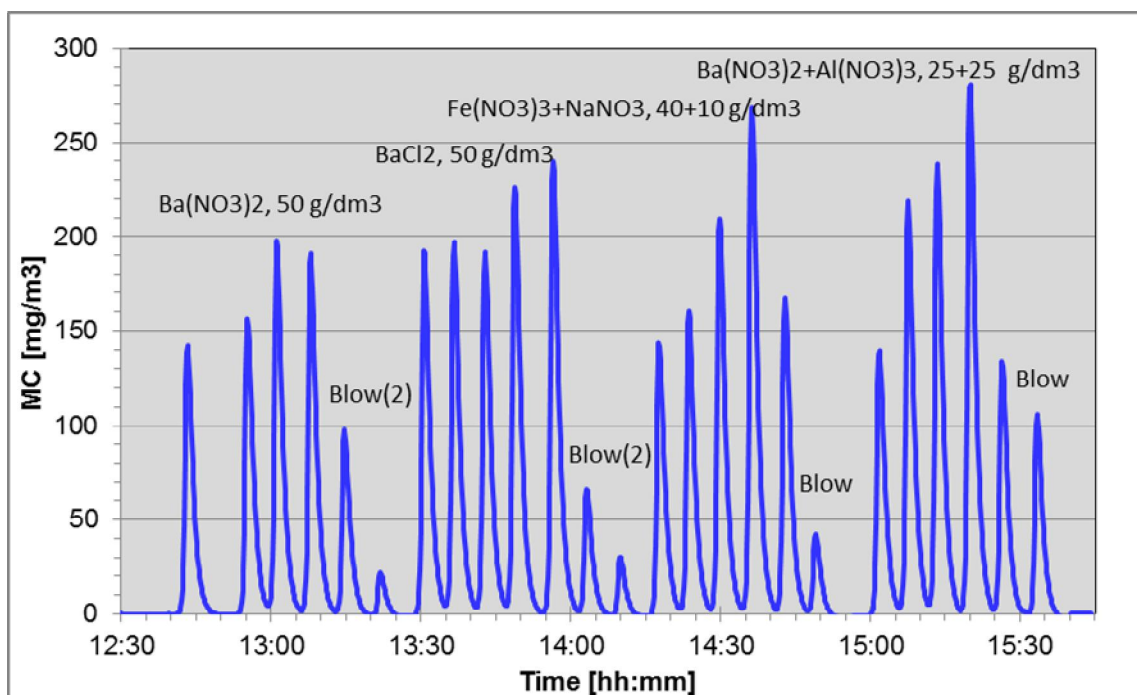


Fig. 29. Particle mass concentration for $\text{Ba}(\text{NO}_3)_2$, BaCl_2 , $\text{Ba}(\text{NO}_3)_2 + \text{Al}(\text{NO}_3)_3$ and $\text{Fe}(\text{NO}_3)_3 \cdot 9\text{H}_2\text{O} + \text{NaNO}_3$ reagents measured with TEOM on **1.9. 2011** (see Fig. 25). The particles are collected (collection time 5 min) on a filter, and pulses generated by a powerful “blow” of air (10 bar) through the filter. “Blow” indicates “blowing” air through the filter without any collection of the particles.

3.2.2.3 Particle morphology

The collecting filter element after the experiment on **1.9.2011** ($\text{Ba}(\text{NO}_3)_2$, BaCl_2 , $\text{Ba}(\text{NO}_3)_2 + \text{Al}(\text{NO}_3)_3$ and $\text{Fe}(\text{NO}_3)_3 \cdot 9\text{H}_2\text{O} + \text{NaNO}_3$ reagents, Fig. 30) did not look like condensation of possibly water vapour had occurred. The different colour of the collected particles was clearly visible (the deep orange originating from $\text{Fe}(\text{NO}_3)_3 \cdot 9\text{H}_2\text{O}$ and the white from other reagents)

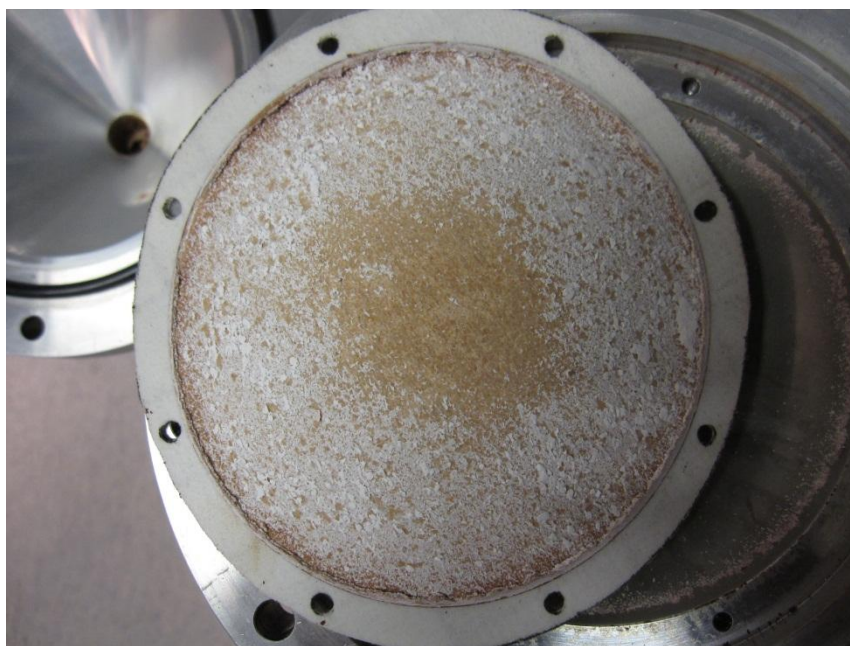


Fig. 30. The collecting side of the filter after the experiment on **1.9.2011** used for collecting particles produced from $\text{Ba}(\text{NO}_3)_2$, BaCl_2 , $\text{Ba}(\text{NO}_3)_2 + \text{Al}(\text{NO}_3)_3$ and $\text{Fe}(\text{NO}_3)_3 \cdot 9\text{H}_2\text{O} + \text{NaNO}_3$ reagents.

The individual particle samples were collected with an aspiration electron microscopy sampler (AEM sampler). With $\text{Ba}(\text{NO}_3)_2$ reagent (50 g/dm^3) during normal pulsed generation the particles (collection with a new filter) majority of the particles were mainly aggregates of different sizes (up to about few μm). However, single spherical and rod-like particles were also found (Fig. 31a). Indication of sintering/fusion of the particles was also discovered (Fig. 31 b). This may have been also caused by water condensation.

For BaCl_2 (50 g/dm^3) reagent the majority of the particles were aggregates of different sizes, usually smaller than approximately $2 \mu\text{m}$ (Fig. 31c). Also the degree of agglomeration varied: some of the particles consisted of many very small particles ($\leq 100 \text{ nm}$), some nearly $1 \mu\text{m}$ sized particles (Fig. 31d).

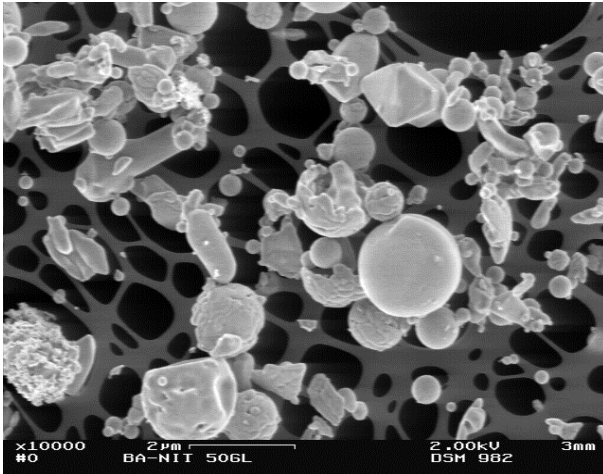


Fig. 31a. The generated particles with $\text{Ba}(\text{NO}_3)_2$ reagent (1.9.2011) collected with a filter and “blown” away. Particles were, generally smaller than $2\ \mu\text{m}$, but of different shapes.

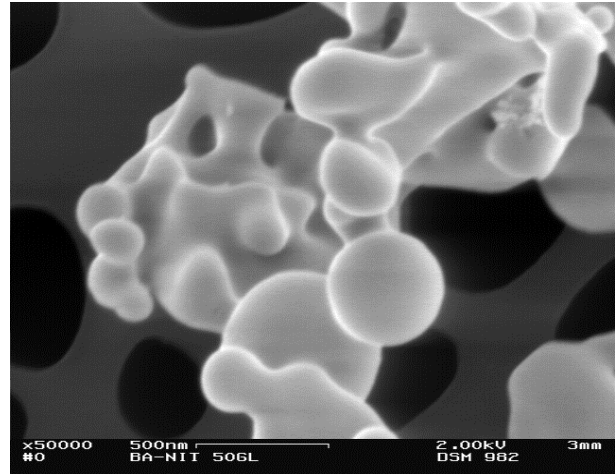


Fig. 31b. A detail of the collected particle. Indication sintering/fusion of the particles together was found.

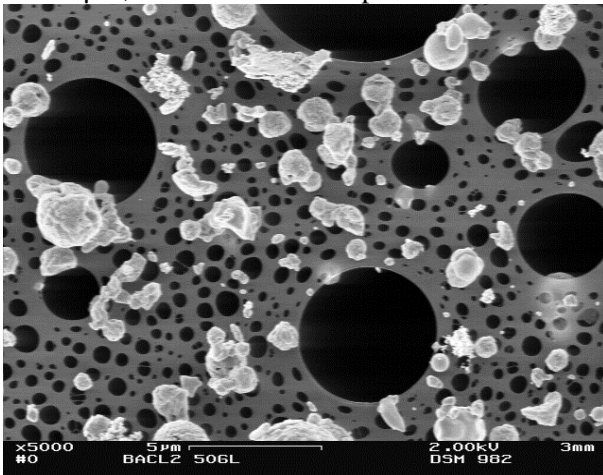


Fig. 31c. The generated particles with BaCl_2 reagent (1.9.2011) collected with a filter and “blown” away.

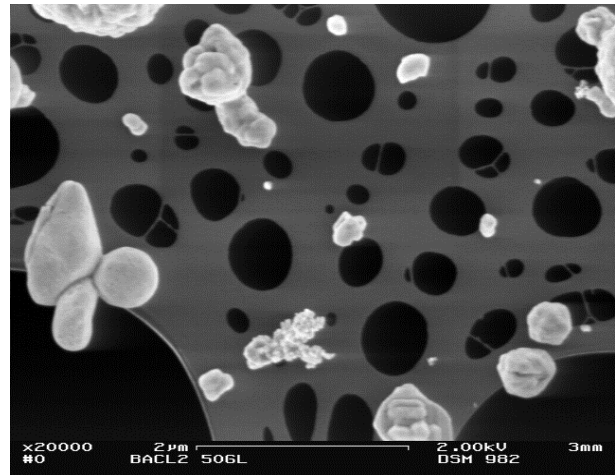


Fig. 31d. A detail of the collected particles. Particles are generally different sized aggregates with different degree of agglomeration.

For $\text{Fe}(\text{NO}_3)_3 \cdot 9\text{H}_2\text{O} + \text{NaNO}_3$ ($25+25\ \text{g}/\text{dm}^3$) reagent during normal pulsed generation the particles (collection with a new filter) many different sized particles were found: spheres, rods, rectangles and aggregates of these (Fig. 32b). Majority of the particles were smaller than about $2\ \mu\text{m}$ (Fig. 32a). Despite of the high degree of agglomeration single spherical and rod-like particles were also found (Fig. 31b). No indication of sintering/fusion of the particles was discovered.

For $\text{Ba}(\text{NO}_3)_2 + \text{Al}(\text{NO}_3)_3$ ($25+25\ \text{g}/\text{dm}^3$) reagent particles were generally aggregates generally smaller than a few μm in size (Fig. 32c). In addition, single almost spherical particles smaller than approximately $1\ \mu\text{m}$ were also found (Fig. 32d).

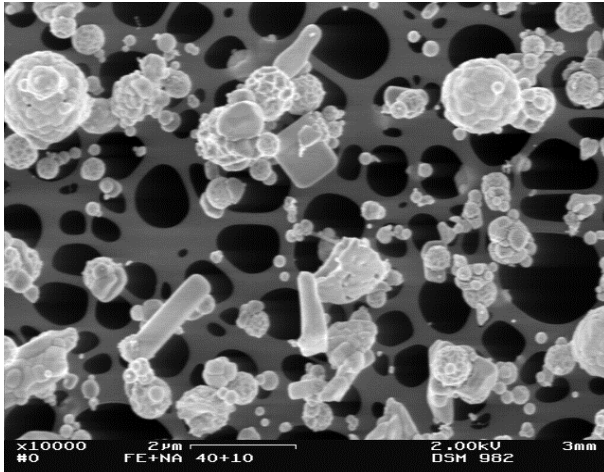


Fig. 32a. The generated particles with $\text{Fe}(\text{NO}_3)_3 \cdot 9\text{H}_2\text{O} + \text{NaNO}_3$ reagent (1.9.2011) collected with a filter and “blown” away. Particles are, generally smaller than $2 \mu\text{m}$.

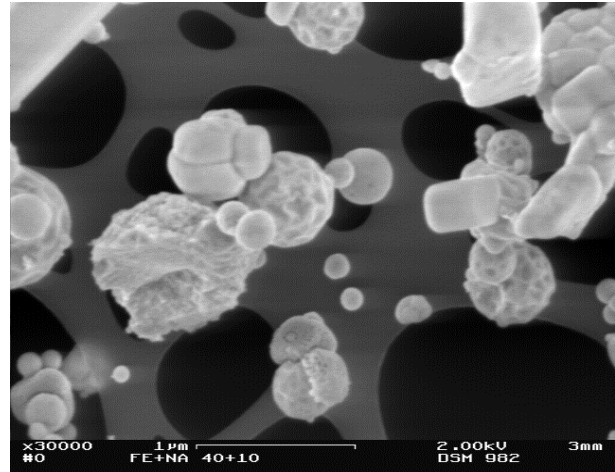


Fig. 32b. A detail of the collected particles. A lot of different shaped particles were found: spheres, rods, rectangles and aggregates of these.

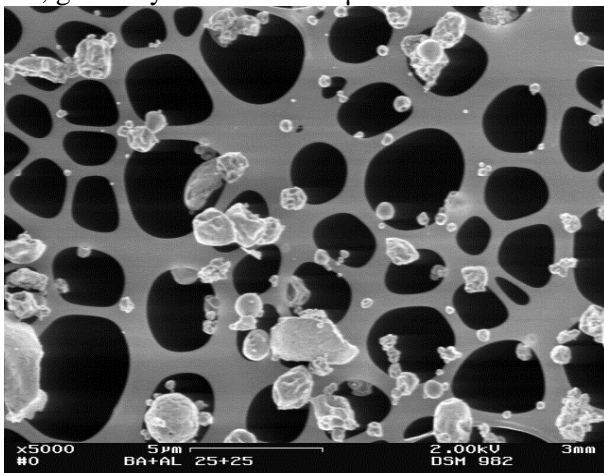


Fig. 32c. The generated particles with $\text{Ba}(\text{NO}_3)_2 + \text{Al}(\text{NO}_3)_3$ reagent (1.9.2011) collected with a filter and “blown” away.

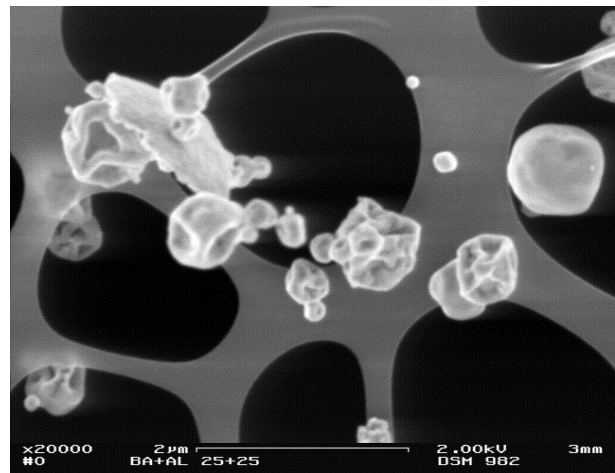


Fig. 32d. A detail of the collected particles. Particles were generally aggregates, but single almost spherical particles were also found.

4 Summary and conclusions

The IndMeas flow calibrator device (FCD) normally using a cyclone for the collection of produced particles was studied and the produced particles characterised. In this study, though, the cyclone was either removed completely to allow the produced particles directly enter the measurement system (campaign 11/2010) or the particles were collected on the surface of a new filter and removed by a fast and powerful “blow” similar as in the case of the cyclone (campaign 9/2011).

During the first campaign (11/2010) different concentrations of $\text{Fe}(\text{NO}_3)_3 \cdot 9\text{H}_2\text{O}$ reagent were studied: 20 g/dm^3 , 40 g/dm^3 and 80 g/dm^3 with and without added silica. As expected, the more concentrated the reagent solution, the higher the particle number and mass concentration. The addition of silica increased the number concentration significantly, from 4 to 10 times higher than without silica. As an example, 20 g/dm^3 the number concentration varied between $3.0\text{-}4.0 \cdot 10^5 \text{ 1/cm}^3$, and the aerodynamic count median diameter (CMD_{ae}) of the particles varied between 70-100 nm. Based on these “screening studies” it was decided to study

$\text{Fe}(\text{NO}_3)_3 \cdot 9\text{H}_2\text{O}$ 40 g/dm³ in more detail. BaCl_2 was used as a “reference” (currently used in the IndMeas FCD).

The particle number concentration for $\text{Fe}(\text{NO}_3)_3 \cdot 9\text{H}_2\text{O}$ (40 g/dm³, 20 ml/min) reagent varied from $1.5 \cdot 10^6$ 1/cm³ to $0.4 \cdot 10^6$ 1/cm³ thus decreasing as a function of time, and the aerodynamic count median diameter (CMD_{ae}) of the particles varied from 52 to 61 nm. The mass concentration measured with TEOM varied from 11 mg/m³ to 14 mg/m³. **Adding silica** increased the particle number concentration to $3.0 \cdot 10^6$ - $5.5 \cdot 10^6$ 1/cm³, and the CMD_{ae} of the particles varied from 51 to 66 nm. Thus the number concentration was 5-10 times higher than without the added silica. The mass concentration measured with TEOM was approximately 16 mg/m³.

For BaCl_2 reagent the number concentration decreased steadily from $1.7 \cdot 10^6$ 1/cm³ to $0.8 \cdot 10^6$ 1/cm³ being thus roughly about the same as with $\text{Fe}(\text{NO}_3)_3 \cdot 9\text{H}_2\text{O}$ without the silica. The mass concentration measured with TEOM was approximately 9 mg/m³.

The mass size distribution for $\text{Fe}(\text{NO}_3)_3 \cdot 9\text{H}_2\text{O}$ and $\text{Fe}(\text{NO}_3)_3 \cdot 9\text{H}_2\text{O} + \text{silica}$ reagent were almost identical: the mode was at approximately 72 nm sized particles, and major part of the particles were smaller than 1 μm in aerodynamic size (assuming unit density of the particles). For BaCl_2 reagent the particles grew larger, and had a mode at approximately 2.7 μm.

The individual particles for $\text{Fe}(\text{NO}_3)_3 \cdot 9\text{H}_2\text{O}$ reagent were different sized spheres up to about few μm in diameter the smallest being <200 nm in diameter. Adding **silica** caused the particles to be less spherical, and the surface was not as smooth as without silica. For BaCl_2 reagent the produced particles were different sized spheres as in the case for $\text{Fe}(\text{NO}_3)_3 \cdot 9\text{H}_2\text{O}$ reagent. The surface of the spheres was folded and wrinkled, but in a different way as for $\text{Fe}(\text{NO}_3)_3 \cdot 9\text{H}_2\text{O}$: it seemed like the surface had sintered/fused together partly losing its microstructure.

During the second campaign (9/2011) the particles were collected after the production with a new filter sampler instead of a cyclone. The particles were “blown” away from the surface of the filter element by a powerful pulse of air. Many different reagents and reagent combinations were tested: $\text{Fe}(\text{NO}_3)_3 \cdot 9\text{H}_2\text{O}$, $\text{Fe}(\text{NO}_3)_3 \cdot 9\text{H}_2\text{O} + \text{Ba}(\text{NO}_3)_2$, $\text{Ba}(\text{NO}_3)_2$, BaCl_2 , $\text{Ba}(\text{NO}_3)_2 + \text{Al}(\text{NO}_3)_3$ and $\text{Fe}(\text{NO}_3)_3 \cdot 9\text{H}_2\text{O} + \text{NaNO}_3$.

For $\text{Fe}(\text{NO}_3)_3 \cdot 9\text{H}_2\text{O}$ reagent (40 g/dm³, 10 ml/min) the particle number concentration varied between 2.0 - $2.1 \cdot 10^7$ 1/cm³. The aerodynamic count median diameter (CMD_{ae}) of the particles varied approximately between 1-2 μm. The number size distribution for $\text{Fe}(\text{NO}_3)_3 \cdot 9\text{H}_2\text{O}$ reagent during one single pulse was typically unimodal with a peak at approx. 70 nm. Addition of $\text{Ba}(\text{NO}_3)_2$ did not have any significant effects on the particle number concentration or on particle CMD_{ae} .

Typical particle mass concentration for $\text{Fe}(\text{NO}_3)_3 \cdot 9\text{H}_2\text{O}$ reagent varied between 90-220 mg/m³. The lower mass concentration during the first “blow” was probably caused by the filter being clean, i.e. it had not “saturated” and thus some part of the particle mass was trapped in the pores of the filter. Addition of $\text{Ba}(\text{NO}_3)_2$ decreased particle mass concentration to 80-100 mg/m³.

For the following experiments a new filter element was changed. For $\text{Fe}(\text{NO}_3)_3 \cdot 9\text{H}_2\text{O}$ reagent (50 g/dm³, 10 ml/min) and the addition of $\text{Ba}(\text{NO}_3)_2$ either 1 or 10 g/dm³ did not cause any significant changes in number concentration or particle CMD_{ae} compared to previous results for $\text{Fe}(\text{NO}_3)_3 \cdot 9\text{H}_2\text{O}$ reagent. However, the mass concentration varied between 20-40 mg/m³, which was significantly lower than for previous measurements. The much lower total particle mass concentration was afterwards traced to the different filter used in these experiments. The filter used in these experiments must have been of different material, because it was found to have a much worse collection efficiency than the one used on previous experiments: a significant part of the collected particles were able to penetrate through the filter material. Thus these results are not directly comparable with other ones.

The mass size distribution for the normal pulsed particle generation (collection of the particles by a new filter) with $\text{Fe}(\text{NO}_3)_3 \cdot 9\text{H}_2\text{O}$ and $\text{Fe}(\text{NO}_3)_3 \cdot 9\text{H}_2\text{O} + \text{Ba}(\text{NO}_3)_2$ reagent were clearly bimodal, and almost identical independent on the addition of $\text{Ba}(\text{NO}_3)_2$ reagent. The small particle mode was at approximately 70 nm, and “large” particle mode at approximately 6 μm (assuming unit density of the particles, Fig. 21). For comparison, a mass size distributions from previous experiment (11/2010) for $\text{Fe}(\text{NO}_3)_3 \cdot 9\text{H}_2\text{O}$ and $\text{Fe}(\text{NO}_3)_3 \cdot 9\text{H}_2\text{O} + \text{silica}$ reagent with continuous production of particles (no collection device) had a small particle mode at the same location as the ones produced by normal pulsed particle generation (collection of the particles by a new filter). However, the large particle mode at 6 μm was missing. Thus it seems that the particles were agglomerating at the filter collection possibly because of the water condensation at the lower temperature than usual with the cyclone collection during the filter collection of the particles. It should be noted that, unfortunately, these BLPI measurements were carried out with the leaking filter.

Dividing the particles roughly into two particle fractions, under and over 1 μm it was found that during the continuous production of the particles (11/2010) nearly over 60 % of the mass of the particles was found in smaller than 1 μm sized particles. During the normal pulsed particle generation (collection of the particles by a new filter) only 30 % of the mass was found in smaller than 1 μm sized particles. This also indicated that agglomeration at the filter collection possibly because of the water condensation at the lower temperature than usual with the cyclone collection occurred. However, there may also be other causes for agglomeration of the particles.

For $\text{Ba}(\text{NO}_3)_2$ reagent (50 g/dm³) the number concentration varied between 1.0-1.8·10⁷ 1/cm³, and the aerodynamic count median diameter (CMD_{ae}) of the particles varied approximately between 1.8-2.5 μm. For BaCl_2 no significant difference was found. The mass concentration for $\text{Ba}(\text{NO}_3)_2$ was slightly lower than for BaCl_2 (140-200 mg/m³ vs. 190-240 mg/m³).

For $\text{Fe}(\text{NO}_3)_3 \cdot 9\text{H}_2\text{O} + \text{NaNO}_3$ (25+25 g/dm³) reagent the particle number concentration varied between 1.0-1.3·10⁷ 1/cm³, and the particle CMD_{ae} varied approximately between 1.2-2.1 μm. The particle mass concentration varied between 150-270 mg/m³.

For $\text{Ba}(\text{NO}_3)_2 + \text{Al}(\text{NO}_3)_3$ (25+25 g/dm³) reagent the particle number concentration varied between 1.4-1.7·10⁷ 1/cm³, and particle CMD_{ae} varied approximately

between 1.2-2 μm . The particle mass concentration varied between 130-280 mg/m^3 .

As a conclusion, the IndMeas flow calibrator device (FCD) is able to produce small particles ($\ll 1\mu\text{m}$), but it seems the new filter used to collect them causes some agglomeration of the particles into larger ones. This agglomeration at the filter collection could be caused by water condensation at the lower temperature than usual with the cyclone collection. However, there may also be other causes for the agglomeration of the particles. The solution to the agglomeration could be a higher collection temperature or another reagent or a “deagglomerating agent”. Another possibility would be to skip the particle collection phase totally if possible, because it was found that the most severe agglomeration occurred during filter collection. The question to be answered is, is the signal level (radioactive tracer) without any collection of the particles high enough to be separated from the background noise. The signal to noise ratio could be enhanced by using more concentrated reagents. There is a trade-off, however, when increasing the concentration of the reagent solution, the tendency to form agglomerates also increases.

References

- Auvinen, A., Lehtinen, K. E. J., Enriquez, J., Jokiniemi, J. K. and Zilliacus, R. (2000) Vaporisation rates of CsOH and CsI conditions simulating severe nuclear accident. *J. Aerosol Sci.* 31, 1029–1043.
- Baltensperger, U., Weingartner, E., Burtscher, H. and Keskinen, J. (2001) Dynamic mass and surface area measurement. In: *Aerosol Measurement – Principles, techniques and applications* (Edited by Baron, P. A. and Willeke, K.). John Wiley and Sons. Pp. 387–418.
- Berner, A. and Lürzer, C. (1980) Mass size distribution of traffic aerosols in Vienna. *J. Phys. Chem.* 84, 2079–2083.
- Berner, A., Lürzer, C., Pohl, F., Preining, O. and Wagner, P. (1979) The size distribution of the urban aerosol in Vienna. *Sci. Total Environment* 13 (3), 245–261.
- Cheng, Y.-S. (1993) Instrumental techniques/Condensation detection and diffusion size separation techniques. In: *Aerosol Measurement – Principles, techniques and applications* (Edited by Willeke, K. and Baron, P. A.). New York: Van Nostrand Reinhold. Pp. 427–451.
- Cleen MMEA factsheet (Dec 2010). Measurement, monitoring and environmental assessment – innovations through new thinking.
http://www.cleen.fi/home/sites/www.cleen.fi/home/files/Cleen_Factsheet_MMEA_final.pdf.
- Hillamo, R. E. and Kauppinen, E. I. (1991) On the performance of the Berner Low-Pressure Impactor. *Aerosol Sci. Technol.* 14, 33-47.

Kauppinen, E. I. (1992) On the determination of continuous submicrometer liquid aerosol size distributions with low-pressure impactors. *Aerosol Sci. Technol.* 16, 171-197.

Keskinen, J., Pietarinen, K. and Lehtimäki, M. (1992) Electrical low-pressure impactor. *J. Aerosol Sci.* 23, 353-360.

Lyyränen, J., Laukkanen, V., Ahlfors, K. and Auvinen, A. (2011) Characterisation of the produced particles by the IndMeas industrial flow calibration device. VTT research report VTT-R-04408-11, 25 p.

Patashnick, H. and Rupprecht, G. (1986) Advances in microweighing technology. *Am. Lab.* 18, 57-60.

Patashnick, H. and Rupprecht, G. (1991) Continuous PM-10 measurements using the tapered element oscillating microbalance. *J. Air Pollution Control Assoc.* 41, 1079-1083.